universität wien

MASTERARBEIT / MASTER'S THESIS

Titel der Masterarbeit / Title of the Master's Thesis

„Expression of *HES* and *Mox* genes in a polyplacophoran mollusc: New insights into genetic regulation of molluscan mesoderm development."

verfasst von / submitted by

Attila Placido Sachslehner BSc

angestrebter akademischer Grad / in partial fulfilment of the requirements for the degree of

Master of Science (MSc)

Wien, 2020 / Vienna, 2020

Studienkennzahl lt. Studienblatt / degree programme code as it appears on the student record sheet:	A 066 831
Studienrichtung lt. Studienblatt / degree programme as it appears on the student record sheet:	Masterstudium Zoologie UG2002
Betreut von / Supervisor:	Univ.-Prof. DDr. Andreas Wanninger

Index

Abstract **1**

Introduction **2**

Material and Methods **5**

Animals and fixation 5

RNA probes design 6

In situ hybridisation 8

Phylogeny and bioinformatics 11

Gene annotation trees 11

Results **13**

Identity of genes of interest 13

Myosin heavy chain (*MHC*) 13

Mox 13

Hairy and enhancer of split (*HES*) 14

Expression patterns of target genes 14

Myosin heavy chain (*MHC*) 14

Mox 15

Hairy and enhancer of split (*HES*) 16

Discussion **17**

Myosin heavy chain (*MHC*) expression in metazoans 17

Mox gene expression in metazoans 19

Hairy and enhancer of split (*HES*) gene expression in metazoans 22

Conclusion **26**

Acknowledgements **27**

Figures **28**

Tables **40**

References **44**

Zusammenfassung **57**

Abstract

The mesoderm is argued to be the youngest of the three germ layers that probably evolved after the cnidarian-bilaterian split. Although its morphogenesis has been studied in numerous metazoans, the molecular components underlying this process remain unknown in the majority of phyla including the highly diverse Mollusca. Here, expression of *hairy and enhancer of split* (*HES*) and *Mox* were investigated in the polyplacophoran mollusk *Acanthochitona*, together with a common regulator in animal myogenesis, *Myosin heavy chain* (*MHC*). *AcaMHC* is expressed during myogenesis in the early larva as well as in muscles of the late larva and the juvenile. *AcaMox1* is expressed in the mesodermal bands and in the ventrolateral muscle, an apomorphic feature of the polyplacophoran trochophore. Two of the seven annotated *AcaHES* genes yielded results by in situ hybridization. *AcaHESC2* is expressed in the ectoderm of the gastrula, the mesodermal bands and in putative developing neuronal tissue of the late trochophore larva. *AcaHESC7* is expressed in the trochoblasts of the gastrula and during foregut formation. *AcaMox1* expression in the mesodermal bands is similar to other lophotrochozoans such as the gastropod *Haliotis asinina*, the brachiopod *Terebratalia transversa*, and the annelid *Alitta virens*. A metazoan-wide comparison reveals *Mox* expression in the mesoderm in numerous bilaterians (except echinoderms) and in the cnidarian endoderm. In addition, *Mox* is involved in myogenesis in molluscs, annelids, urochordates, and craniates but not in *Drosophila* while nematodes have lost a *Mox* ortholog altogether. *HES* genes are expressed during a number of developmental processes such as segmentation, neurogenesis, and gut formation, providing evidence that so-called “mesodermal genes” are not confined to mesoderm formation alone. Further studies are needed to fully understand the molecular pathways underlying bilaterian mesoderm development and evolution.

Introduction

Germ layers form early in animal embryonic development and are the precursors of adult tissues and cell types such as neurons or muscles. The evolutionary older two germ layers, the ectoderm and the endoderm, are established during gastrulation. The third germ layer, the mesoderm, is argued to be the youngest that probably evolved in the bilaterian lineage (Technau and Scholz, 2003; Chiodin et al., 2013; Passamaneck et al., 2015; Salinas-Saavedra et al., 2018; but see Martindale, 2004; Burton, 2008 for alternative view). In a number of protostomes, the mesoderm is formed by cells that immigrate from the blastopore margin into the blastocoel, sometimes forming a pair of mesodermal bands as, for example, in the spiralians (Boyer et al., 1996; Van Den Biggelaar, 1996; Fischer and Arendt, 2013; Seaver, 2014; Wanninger and Wollesen, 2015). In deuterostomes and some protostomes, the mesoderm-forming cells typically detach from the archenteron wall (Minguillón and Garcia-Fernàndez, 2002; Technau and Scholz, 2003; Lowe et al., 2006). The mesoderm is often considered a major innovation since key organ systems such as muscles or connective tissue derive from this germ layer (Kozin et al., 2016).

In lophotrochozoans with spiral cleavage (e.g. Mollusca, Annelida, Plathyhelminthes), a major fraction of the mesoderm forms from a distinct progenitor cell, the so-called mesentoblast or 4d cell, as a pair of lateral bands (Boyer et al., 1996; Van Den Biggelaar, 1996; Fischer and Arendt, 2013). The genealogy of the second source of the mesoderm, the mesectoblast, varies within the spiralians and may derive from micromeres of the first, second, and/or third quartet (Conklin 1897; Holmes 1900; Boyer et al. 1996). While the mesodermal cell lineage has been investigated in a number of lophotrochozoan representatives including the flatworm *Hoploplana* (Boyer et al., 1996), the polychaete annelids *Podarke*, *Polygordius*, and *Scoloplos* (Anderson, 1973), the gastropods *Planorbis* (Holmes 1900) and *Crepidula* (Conklin, 1897), and the polyplacophoran mollusk

Acanthochitona (Van Den Biggelaar, 1996), the molecular mechanisms underlying mesoderm specification remain largely unclear (Wanninger and Wollesen, 2015). *Myosin heavy chain* (*MHC*), *Mox*, and *Hairy and enhancer of split* (*HES*) genes are known to be expressed in mesoderm and/or early muscle formation in several bilaterians (Zhang and Bernstein, 2001; Thamm and Seaver, 2008; Passamaneck et al., 2015; Brunet et al., 2016; Kozin et al., 2016; Schiemann et al., 2017) and were tested here for potential involvement in mesoderm formation in an emerging mollusk model, the polyplacophoran *Acanthochitona*.

MHC or *myosin class II* is a member of the myosin super family. It is, together with *myosin class I*, often assumed to constitute the most ancient myosin class that already evolved at the bikont-unikont split (Richards and Cavalier-Smith, 2005). The protein products of *MHC* build the myosin fibres found in the muscle cells of bilaterians (Wells et al., 1996; Thompson and Langford, 2002). In the annelid *Platynereis dumerilii*, *PduMHC* is expressed in both striated and smooth muscles of the early nectochaete larva. Other stages were not investigated (Brunet et al., 2016). In *Drosophila melanogaster, MHC* (*DmeMHC*) starts to be expressed when the germ band retracts and segment formation starts (stage 12). Expression lasts until completion of head involution and the start of cuticle secretion (stage 15-16) (Hartenstein and Chipman, 2015). During this developmental phase, *DmeMHC* is expressed in somatic and visceral muscles as well as in cardioblasts (Zhang and Bernstein, 2001). In the echinoderm *Strongylocentrotus purpuratus*, a MHC protein is first expressed in the late gastrula and in the pluteus larva (Andrikou et al., 2015). In the cephalochordate *Branchiostoma belcheri*, *MHC* (*BbeMHC*) expression is found during somite formation and in the notochord (Suzuki and Satoh, 2000; Urano et al., 2003), while in vertebrates, *MHC* is involved in development of skeletal, cardiac, and smooth muscles (McGuigan et al., 2004). In the non-bilaterian cnidarian *Nematostella MHC* (*NveMHC*) transcripts are

present in the tentacle muscles and in retractor muscles of primary polyps (Renfer et al., 2010).

Mox belongs to the homeotic genes, which possess a conserved helix-turn-helix DNA-binding homeodomain. Previous studies have suggested a sister group relationship to the homeotic gene *even-skipped* also referred to as *Evx*. *Mox* and *Evx* are proposed to have a common ancestor which was linked to the ProtoHox cluster (Minguillon and Garcia-Fernandez, 2003). It has been argued that a large-scale tandem duplication gave rise to the coupled Hox and ParaHox cluster that included *Mox* and *Evx* early in metazoan evolution (Pollard and Holland, 2000). A chromosomal breaking event of the coupled Hox- and ParaHox cluster isolated the primordial ParaHox cluster from the extended Hox cluster that include *Evx* and *Mox* (Banerjee-Basu and Baxevanis, 2001). Expression of *Mox* orthologs in the ventral mesoderm in the fly *Drosophila melanogaster* (Chiang et al., 1994), the gastropod *Haliotis asinina* (Hinman and Degnan, 2002), the brachiopod *Terebratalia transversa* (Passamaneck et al., 2015), and the polychaete *Alitta virens* (Kozin et al., 2016) suggests a conserved expression pattern within protostomes. In chordates, *Mox* expression was reported for example during somite formation and differentiation, which are sequential segments that originate from the dorsal paraxial mesoderm and subsequently form muscles, bones, and connective tissue (Candia et al., 1992; Minguillón and Garcia-Fernàndez, 2002). *Mox* expression in muscle progenitors and muscle tissue in *Haliotis* (Hinman and Degnan, 2002), *Alitta* (Kozin et al., 2016) and vertebrates (Candia et al., 1992) suggests a putative ancestral role of *Mox* in early myogenesis in bilaterians. Expression of the *Drosophila Mox* ortholog *buttonless* is restricted to dorsal median cells. These play a crucial role in axon guidance in *Drosophila*. *Buttonless* expression was not detected in *Drosophila* muscle progenitor cells or muscle tissue (Chiang et al., 1994), suggesting a loss of *Mox* in myogenesis. Nematodes have lost a *Mox* ortholog altogether (Ruvkun et al., 1998).

HES genes are members of the basic helix-loop-helix superfamily and direct downstream targets of the Delta-Notch signalling pathway (Iso et al., 2003). They possess an additional *HES* specific hairy orange domain (after the basic-helix-loop-helix domain) and a WRPW motif at the C-terminal end (Thamm and Seaver, 2008). The origin of *HES* genes is thought to have been in the last common metazoan ancestor (Simionato et al., 2007). They are involved in a variety of developmental processes such as maintaining stem cell potential or partitioning of morphological territories (i.e. segmentation in annelids, arthropods, chordates as well as in budding in *Hydra*) (Minguillón et al., 2003; Kageyama et al., 2007; Thamm and Seaver, 2008; Münder et al., 2010; Gazave et al., 2014). *HES* genes in mollusks have so far only been studied in the gastropod *Crepidula fornicata*, where one *HES* gene was found to be expressed around the mouth as well as in neurosensory cells in the early larva, while the other one shows more dynamic expression domains in the lateral ectoderm around the mouth (Perry et al., 2015).

Herein, expression of the muscle marker gene *MHC* and the two putative "mesodermal" genes *Mox* and *HES* were studied in the polyplacophoran mollusk *Acanthochitona* to assess whether *Mox* and *HES* are likely to play a role in molluscan mesoderm formation as suggested for other lophotrochozoans and bilaterians.

Material and Methods

Animals and fixation

According to CO1 blasts, the used polyplacophoran species belongs to *Acanthochitona crinita* but it might be another species according to unpublished data. Herein, the model organism is referred to as *Acanthochitona*. Adult *Acanthochitona* specimens were collected in the intertidal between the Station Biologique de Roscoff and Île Verte in Roscoff, France

(48°43′44.70”N 3°59′13.53”W). Adults and all developmental stages were maintained in glass dishes with filtered seawater at 18-21°C. Spontaneous spawning generally occurred one to three days after adults had been brought to the lab. Gametes were collected immediately and in vitro fertilization was carried out by adding several drops of sperm to the eggs. Upon the first observation of 2-cell stages (~80 minutes after fertilization), eggs were washed multiple times with filtered sea water to prevent polyspermy. The gastrula stage of development was reached at about 8 hours post fertilization (hpf). Trochophore larvae hatched at about 18 hpf. At 48 hpf larvae reached the metamorphic competent stage (referred to as “late trochophore larva” herein). Early juveniles that had completed metamorphosis appeared between 60-90 hpf.

In order to fix samples for RNA extraction, specimens were centrifuged, the seawater was removed and liquid nitrogen was added. Specimens were stored at -80°C until RNA extraction could proceed. For in situ hybridization experiments, specimens were fixed for 1-2 hours in 4% paraformaldehyde (PFA Sigma-Aldrich #158127; St. Louis, USA) in MOPS-EGTA (0.1M MOPS Sigma-Aldrich #69947; 2mM $MgSO_4$ Thermo Fisher Scientific #52044; Waltham, USA); 1mM EGTA, Sigma-Aldrich #E4378; 0.5M NaCl, Roth #HN00.1; Karlsruhe, Germany), and washed twice or thrice in ice cold 100% methanol. Fixed specimens were stored at -20°C.

RNA probes design

Total RNA extraction from 12 pooled developmental stages, from early cleavage stages to juveniles, was performed using the Qiagen RNeasy mini kit 50 (#74104; Venlo, Netherlands). Reverse transcription into cDNA was performed with the Roche 1st strand cDNA synthesis kit for RT_PCR (Roche #11483188001; Rotkreuz, Switzerland). Specific

primers for each gene of interest were designed manually and purchased from Microsynth AG (Zürich, Switzerland) (Table 1). Reading frames and orientation of the transcriptomic templates were assessed with the ExPASy translate tool (Artimo et al., 2012; https://web.expasy.org/translate/). All transcriptomic templates are in sense frame. Melting temperatures of designed primers were assessed with the Promega Oligo Calculator tool (Rychlik and Rhoads, 1989; https://at.promega.com/resources/tools/biomath/tm-calculator/; 500nM primer concentration, 5x green or colourless GoTaq® Reaction Buffer) and self-complementary check was done with the Northwestern biotools OligoCalc tool (Kibbe, 2007; http://biotools.nubic.northwestern.edu/OligoCalc.html). The genes of interest were amplified by PCR (Promega protocol #9PIM829; 5x Go Taq Flexi Buffer Promega #M890A (Fitchburg, USA); magnesium chloride, Promega #A351; dNTP Mix, Promega #1141; Go Taq Flexi DNA Polymerase, Promega #M780B) and the gene specific primers. The amplified genes were ligated into a pGEM-T easy vector (Promega #A1380). The plasmid was transformed into *E. coli* competent cells (Promega #L2001). Transformed bacteria were grown overnight at 37°C on LB agar plates (Promega: 10g/l Bacto®-tryptone; 5g/l Bacto®-yeast extract; 5g/l NaCl, Roth #HN00.1; pH = 7) containing IPTG (Promega #V3955), XGal (Promega #V3941), and ampicillin (1000x, Sigma #A9518) followed by the selection of positive colonies through blue/white colony screening. White colonies were picked and grown over night in cloning cylinders with 5ml LB medium. Confirmation of successful transformation of the colonies were performed by PCR (Promega #9PIM829) using plasmid specific M13 forward (Promega #Q5601) and reverse (Promega #Q5421) primers (Steffens et al., 1993). Plasmid DNA was purified using the QIAprep spin miniprep kit 250 (Qiagen #27106). Inserts were sequenced by Microsynth AG (Vienna) using sp6 primers. Insert orientation was determined by aligning the sp6-primed sequence to the original transcript and this information was used to determine the appropriate RNA

polymerase for sense and antisense RNA probe synthesis. Amplification of the insert was done by PCR (Promega protocol #9PIM829; M13 Primer, Microsynth AG). In vitro transcription was done using the DIG RNA Labeling Mix, 10x conc. (Roche #11277073910) with either T7 RNA polymerase (Roche #10881767001) or sp6 RNA polymerase (Roche #10810274001). Additionally, 1µl of DTT (Sigma-Aldrich #D0632) was added to each sample and incubation was performed for three instead of two hours to increase the RNA probe yield. The RNA probes were sephadex-purified using the Illustra ProbeQuant G-50 Micro Columns (GE Healthcare Life sciences #28903408; Pittsburgh, USA) and precipitated over night at -20°C (4M LiCl, Sigma-Aldrich #L7026; 96-100% ethanol). Precipitated probes were washed twice for 15 minutes in 70% ethanol, airdried at room temperature, and dissolved in 20µl nuclease-free water (Thermo Fisher Scientific #R0581). The probes were stored at -80°C.

In situ hybridisation

Fixed and stored *Acanthochitona* specimens were incubated in EGTA in methanol (90% methanol; 0.05M EGTA pH 8) in order to keep the RNA intact via chelating it. Subsequently, the EGTA solution was stepwise exchanged in an ascending (20%, 50%, 50%, 80%, 100%) phosphate buffered saline series (Roth #1058.1) with 0.1% Tween20, (Roth #9127.1; "PBT"). Specimens were then incubated for a maximum of 2 hours in PPE (PBT; 0.05M EGTA pH 8; 4% PFA) for decalcification and were subsequently washed thrice for 10 minutes each in PBT. Specimens were incubated in a solution of 50µg/ml proteinase-K in PBT (Roche #03115879001) for 10 minutes at 37°C and then washed twice for five minutes each and twice for 10 minutes each in PBT at room temperature. In order to reduce charged probe binding, specimens were subsequently incubated for 10 minutes each in 1% triethanolamine (PBT with 1% TEA added; Sigma-Aldrich #90279), for five

minutes each in 1% TEA with 0.15% acetic anhydride (Prolabo #21390293; Bern, Switzerland) and for five minutes each in 1% TEA with 0,3% acetic anhydride added. Specimens were then washed twice for five minutes each and twice for 10 minutes each in PBT and post-fixed in 4% PFA for 45 minutes. Afterwards, the specimens were washed twice for five minutes each and twice for 10 minutes each in PBT and were incubated in hybridization buffer (50% formamide, Roth #P040; 5x saline sodium citrate SSC, Roth #10541; 100µg/ml heparin, Sigma-Aldrich #H3149; 5mM EDTA, Roth #80401; Denhardts block reagent, Sigma-Aldrich #D2531; 100µg/ml yeast tRNA, Sigma-Aldrich #R675; 0.1% Tween20; 5% dextransulfate, Sigma-Aldrich #D8906) for 10 minutes at room temperature and additionally for approximately 24 hours at 60-62°C in a water bath. Complementary antisense probes and sense probes (0.5-2ng/µl) were preheated in 300µl 100% hybridization buffer for 10 minutes at 85°C. One RNA probe per specimen patch was added and hybridization happened at 60-62°C for approximately 24 hours. Next, the specimens were washed thrice for 20 minutes each in 4x Wash (50% Formamide; 4x SSC; 0.1% Tween20), twice for 20 minutes in 2x Wash (50% Formamide; 2x SSC; 0.1% Tween20) and twice for 15 minutes each in 1x Wash (50% Formamide; 1x SSC; 0.1% Tween20). Subsequently, specimens were washed thrice for 10 minutes each in SSCT (1x SSC; 0.1% Tween20) and then washed four times for 10 minutes each in 0.1M maleic acid buffer (MAB) (0.1M MAB pH 7.5 Sigma-Aldrich #M0375; 0.15M NaCl; 0.1% Tween20). To prevent unspecific anti-digoxigenin antibody binding, specimens were incubated for two hours in 2% MAB block solution (0.08M MAB, pH 7.5; 2% block reagent #11096176001). Afterwards, specimens were incubated in anti-digoxigenin antibody, conjugated to an alkaline phosphatase enzyme (1:5000; Roche #11093274910) in 2% MAB block solution overnight at 4-7°C. Alkaline phosphatase enzyme requires a pH of 9.5 to function, thus a respective alkaline phosphatase buffer (AP) was used (0.5M Tris pH 9.5,

Roth #4855.1; 0.5M NaCl). Next, the specimens were washed four times for 10 minutes each in PBT and further washed thrice for 10 minutes each in alkaline phosphatase buffer (AP; 0.1% Tween20). Signal was developed with a staining buffer (1x AP-buffer; 3.75µl/ml BCIP, Roche #11383221001; NBT 5µl/ml, Roche #11383213001) or, alternatively, with a staining buffer that contained 7.5% polyvinyl alcohol (1x AP-buffer without Tween20 but with 75mg/ml polyvinyl alcohol, Sigma-Aldrich #P1763; 3.75µl/ml BCIP; NBT 5µl/ml). Staining time ranged from 20 to 30 minutes in case of *MHC* and from 3 to 4 hours in case of *Mox*, *HESC2*, and *HESC7*. In case of *HESC1* and *HESC3-C6*, staining was additionally performed over a longer time period, ranging from 16-23 hours of staining. Sense probe specimens were either incubated as long as the antisense specimens, or for two hours longer to check for unspecific signal. If no sense signal was obtained after the additional two hours and the staining was identical in experimental replicates, the antisense signal was considered specific. Signal development was stopped by washing the specimens twice for five minutes each in AP-buffer and thrice for 10 minutes each in PBT. Then the specimens were post-fixed in 4% PFA for 30 minutes each and subsequently washed twice for five minutes each and twice for 10 minutes each in PBT. Specimens were stored in 50% glycerol (Roth #3783.1) diluted in PBT. Prior to clearing, specimens were washed twice for 10 minutes each in an ascending DEPC series in PBT (20%, 40%, 60%, 80%, 100%) and afterwards twice for 10 minutes each in an ascending ethanol series in DEPC (20%, 40%, 60%, 80%, 100%). Specimens were mounted on glass slides and cleared in 2:1 benzylbenzoate:benzylalcohol (Sigma-Aldrich #B9550 and #402834). Specimens were studied with an Olympus BX53 light microscope (Olympus, Tokio, Japan) and images were taken with a DP73 camera (Olympus). Images were manipulated with Fiji (Schindelin et al., 2012).

Phylogeny and bioinformatics

The *Acanthochitona* transcriptome (De Oliveira et al., 2016; available as *Acanthocithona crinita*) was downloaded (https://zoology.univie.ac.at/open-data/) and de-duplicated using cd-hit (Version 4.7), setting the sequence identity threshold to 0.95 (Li and Godzik, 2006; Fu et al., 2012). Corresponding sequences from other mollusks and lophotrochozoans were downloaded from NCBI GenBank (https://www.ncbi.nlm.nih.gov/) and were used as query for the annotation (Table 2, 3, 4). Identification of candidate genes was performed with blastp (Version 2.8.1+) (Altschul et al., 1990) using previously annotated genes from other species as queries (table 2, 3, 4) with the e-value set to e = 1e-6. Annotated genes were reciprocally blasted (blastp) against the NCBI GenBank database using default options to confirm their identity. The annotated sequences were blasted against the Pfam database https://pfam.xfam.org/ to assess whether the expected protein domains were present and complete. In case of the *HES* genes a hmm search (Version 3.1b2) (Eddy, 1995) was performed with the *HES* family specific hairy orange domain as query (Pfam code: PF07527.13). The hairy orange hmm file (Pfam code: PF07527.13) was downloaded from the Pfam database. Seven *HES* gene candidates turned out to possess a complete basic helix-loop-helix domain, a hairy orange domain, and the WRPW motif and these were used for further analysis.

Gene annotation trees

To obtain additional *HES* sequences, the *Crassostrea gigas* Ensembl peptide file (Wang et al., 2012) (https://metazoa.ensembl.org/index.html) was queried with hmmsearch (Version 3.1b2) from the HMMER package (Eddy, 1995) using the Pfam HES hidden markov model (Pfamcode: PF07527.13), yielding six *HES* genes (Table 4). Further, the *Nematostella vectensis* peptide file (Putnam et al., 2007; Sullivan et al., 2008) yielded seven *myosin*

sequences (Table 2) of a non-bilaterian representative. The myosin head domain hmm file (Pfam code: PF00063.21) was downloaded and used as query for the hmm search. High accuracy multiple sequence alignments were calculated using mafft (Version 7.397) (Katoh et al., 2002) with the parameters --maxiterate set to 1000 and --localpair. Alignments were trimmed using BMGE (Version 1.12) (Criscuolo and Gribaldo, 2010) by setting the entropy-like value of the blosum matrix to -BLOSUM30, the maximum entropy threshold to 1, and the minimum length of selected regions to 1. The models for amino acid replacement were calculated using prottest (Version 2.1) (Abascal et al., 2005; Darriba et al., 2017). All available matrices were included (-all-matrices) and models with rate variation among sites (-all-distributions) were included. The likelihood of the predicted models was assessed with the Akaike information criterion (-sort A) (Akaike 1973). Selected amino acid substitution models were LG (Le and Gascuel, 2008) for *MHC* and *HES*, and WAG (Whelan and Goldman, 2001) for *Mox*. Maximum likelihood trees, Bootstrap analyses (100 bootstraps, -b 100) were performed using phyml (Version 20120412) (Guindon and Gascuel, 2003). Tree topology (t), branch length (l), and rate parameters (r) were optimized (-o tlr). Visualisation and annotation of alignments was performed using aliview (Version 1.0.0.0) (Larsson, 2014), Jalview (version 2.11.0.) (Waterhouse et al., 2009), Gimp 2 (Version 2.8.22) and Inkscape (version 0.92.4). Visualisation and annotation of phylogenetic trees was performed with FigTree (Version 1.4.4.) (Rambaut 2006).

Results

Identity of genes of interest

Myosin heavy chain (*MHC*)

One *AcaMHC* ortholog was found in the *Acanthochitona* transcriptome (Fig. 1A). The annotated *AcaMHC* sequence contains one mysoin head domain and one myosin tail domain. A *MHC*-specific glycine (peptide sequence: idf**G**xdl) insertion within the myosin head domain (Richards and Cavalier-Smith, 2005) confirms the gene identity (Fig. 1B). Phylogenetic analysis was performed with eight other members of the myosin superfamily that are commonly found in metazoans (Fig. 1A). Myosin members which are specific to given taxa were not included in the analysis (Thompson and Langford, 2002). A bootstrap analysis with 100 bootstrap replicates was performed to provide statistical support. *Myosin I* is argued to be an ancient member of the myosin superfamily (Thompson and Langford, 2002). Hence, it was used to root the tree. The annotated *AcaMHC* sequence clusters together with its respective metazoan orthologs. The *MHC* clade is well supported as are the clades of the other myosin family members.

Mox

Within the *A. crinita* transcriptome two *Mox* sequences, referred to as *AcaMox1* and *AcaMox2*, were found, which were nearly identical and may constitute allelic variations due to high heterozygosity. Only *AcaMox1* was used for the phylogenetic analysis and the gene expression study due to the better e-value (*AcaMox1* $e =$ 2e-63 vs *AcaMox2* $e =$ 3e-44). *Mox* genes possess a homeodomain with a glutamic acid site that is specific for *Mox* genes (Fig. 2B). It shares a common origin with *Evx*, another homeotic gene. *Mox* and *Evx* together form the sister group to the Hox class genes (Banerjee-Basu and Baxevanis, 2001). The performed bootstrap analysis with 100 bootstrap replicates supports the clustering of *AcaMox1* and *AcaEvx* with their orthologs (Fig. 2A).

Hairy and enhancer of split (*HES*)

Seven putative *HES* sequences, *AcaHESC1* ("C" is for candidate), *AcaHESC2*, *AcaHESC3*, *AcaHESC4*, *AcaHESC5*, *AcaHESC6*, and *AcaHESC7*, were found in the *Acanthochitona* transcriptome. They belong to the bHLH transcription factors and possess two domains, namely a bHLH domain that contains a *HES* gene-specific proline residue and a Hairy orange domain. In addition, they possess a *HES*-specific WRPW motif at the C-terminal end of their sequence (Fig. 3B). The phylogenetic analysis supports the monophyly of the identified *HES* sequences, which form a sister group relationship to *Hey*-class genes (*Hairy and enhancer of split related with a YRPW motif*, see Fig. 3A). These possess the same above-mentioned two domains and the tetrapeptide with a tyrosine at first position instead of a tryptophan. The third group of genes related to the *HES* family are the *Helt* genes (*Hairy and enhancer of split-related protein Helt*). They only possess the bHLH domain and the Hairy orange domain but lack the specific tetrapeptide at the C-terminal end. The most distantly related gene group *Clockwork orange* was used as outgroup. Similar to the *Helt* genes they only possess the bHLH and the Hairy orange domain.

Expression patterns of target genes

Myosin heavy chain (*MHC*)

No *MHC* expression is found in pre-trochophore stages. In the early trochophore larva, *AcaMHC* expression is first detected during early muscle formation (Fig. 4A-D). *AcaMHC* is expressed in small paired domains in three muscles which are about to form, namely the rectus muscle that spans below the future shell plates in anterior-posterior direction, the enrolling muscle that laterally engulfs the larva and the ventrolateral muscle that lies ventrally and consists of two longitudinal muscle strands (Wanninger and Haszprunar, 2002; Scherholz et al., 2015) (Fig. 4A-D). In the late trochophore larva all muscle systems

are fully formed. In this stage all larval muscles (i.e., muscle systems that do not persist until adulthood), such as the prototroch muscle ring that underlies the prototroch, the paired ventrolateral muscle, the single ventromedian muscle, and the apical grid, are present (Wanninger and Haszprunar, 2002; Scherholz et al., 2015). *AcaMHC* expression is detectable in all of these larval muscles (Fig. 4E-H). Muscles that are maintained and elaborated after metamorphosis are the enrolling muscle, the dorsal longitudinal rectus muscle, seven sets of paired dorsoventral muscles (with the eighth being formed only considerably later in post-metamorphic development), and a set of dorsal transversal muscles that underlie the shell plates (Wanninger and Haszprunar, 2002; Scherholz et al., 2015). Expression of *AcaMHC* is detectable in the enrolling muscle, the rectus muscle, and the dorsoventral muscles (Fig. 4E-H). Relatively weak expression domains are found in the region of the developing dorsal transversal muscles (Fig. 4G, H). In the juvenile polyplacophoran, the larval muscles have disappeared and the muscles of the future adult body plan have elaborated. Accordingly, individual myocytes have concentrated into distinct sets of dorsoventral and transversal muscles. Adult-specific muscles such as the buccal musculature that forms several strands around the mouth and the paired radula retractors have formed (Wanninger and Haszprunar, 2002; Scherholz et al., 2015). The ventrolateral muscle is still partly visible and is reduced during further growth. *AcaMHC* expression is found only in the ventrolateral muscle, the enrolling muscle, the dorsoventral muscles, and in the transversal muscles (Fig. 4I-L). No signal was found in other muscles of the juvenile.

Mox

No *AcaMox1* expression was detected in pre-trochophore stages (Fig. 5A, B). The first *AcaMox1* signal is found in the early trochophore larva where it is expressed in the

developing paired mesodermal band in posterior-anterior direction. Expression extends as two broad lateral domains along the ventral mesoderm in a v-shaped manner (Fig. 5C-F). In the late trochophore larva *AcaMox1* expression is confined to the ventrolateral muscle (Fig. 5G-J). *Mox* expression in the juvenile was not investigated.

Hairy and enhancer of split (*HES*)

Two *HES* genes, *AcaHESC2* and *AcaHESC7*, start to be expressed in the late gastrula stage. Expression of both genes is maintained in early larval stages but only *AcaHESC2* is expressed in the late trochophore larva. Expression of the other five *HES* genes was not found. In the gastrula, *AcaHESC2* is expressed in ectodermal cells (Fig. 6A, B). In the early trochophore larva *AcaHESC2* is expressed in the mesodermal bands. A weaker expression domain extends from the anterior pole of the mesodermal bands into the apical region of the larva where it closes in an inverted u-shaped manner (Fig. 6C-F). In the late trochophore larva, *AcaHESC2* expression is limited to the region of the adult buccal ganglion close to the dorsal ectoderm, where two spot-like expression domains are located (Fig. 6G-J). Expression of *AcaHESC7* is first evidently detected in trochoblasts which surround the gastrula (Fig. 7A, B). In the early larval stage *AcaHESC7* expression is restricted to a domain around the mouth (Fig. 7C, D). Through larval development, *AcaHESC7* expression continues to be expressed around the mouth and in the region of the presumptive foregut and ceases in the late trochophore larva (Fig. 7E-H).

Discussion

Myosin heavy chain (*MHC*) expression in metazoans

AcaMHC expression was first detected in the early *Acanthochitona* trochophore larva. The expression pattern coincides with the formation of the ventrolateral muscle, the enrolling muscle and the rectus muscle (Fig 4A-D). During further development the larva elongates and in the late trochophore all major muscle systems are present, with *AcaMHC* being expressed intensely in all muscles. Metamorphosis in polyplacophorans results in reduction and rearrangement of the larval muscular bodyplan and in elaboration of existing muscular systems (Wanninger and Haszprunar, 2002; Wollesen et al., 2013; Scherholz et al. 2015). In the juvenile, *AcaMHC* expression is found only in the ventrolateral muscle, the enrolling muscle, the dorsoventral muscles, and the transversal muscles (Fig. 4I-L). A study in the annelid *Platynereis dumerilii* reveals that *Platynereis MHC* (*PduMHC*) is expressed in the trunk musculature in the late metatrochophore larva but data are incomplete as to whether or not all muscles express *PduMHC* (Pfeifer et al., 2014). In the planarian *Schmidtea*, expression of *MHC* (*SpoMHC*) is first detected on one side of stage 4 embryos (Cardona et al, 2005a). Stage 4 embryos are characterized by massive cell proliferation and differentiation of major tissues (Cardona et al., 2005b). The lack of morphological landmarks in these early embryos, however, makes it difficult to determine the exact location of the signal. At stage 7, when the cerebral ganglion, the eyes, and the pharynx have formed (Cardona et al. 2005b), *SpoMHC* is expressed in the body wall musculature (Cardona et al., 2005a).

In ecdysozoans, a study in *Drosophila* has shown that different isoforms of the *Drosophila MHC* (*DmeMHC*) gene are expressed in different muscles (Zhang and Bernstein, 2001). Generally, *DmeMHC* expression is from the stage of germ band retraction (stage 12) until onset of cuticle secretion and head involution (stage 15-16). Later stages were not

investigated (Hartenstein and Chipman, 2015). *DmeMHC* expression is first seen in somatic and visceral muscles (*MHC* exon 7a). From stage 15 onwards, *DmeMHC* is expressed in cardioblasts (*MHC* exons 3a, 7a, 9b, 11d) which form the heart. *DmeMHC* expression is observed until stage 16, where it is expressed again in the somatic muscles and in transverse muscles (*MHC* exon 3a and 3b) (Zhang and Bernstein, 2001). In adults of the nematode *Caenorhabditis*, four *MHC* genes were found by immunocytochemistry (*CelMHCA-D*). *CelMHCA-B* are expressed in the pharyngeal region, whereas *CelMHCC-D* expression is restricted to body wall muscles (Mackenzie et al., 1978; Bejsovec and Anderson, 1988).

In deuterostomes, a MHC protein (*Spu*MHC) of the echinoderm *Strongylocentrotus purpuratus* is first expressed in the late gastrula in myoblasts that appear in the coelomic sacs at the tip of the archenteron. *Spu*MHC protein expression was investigated until the pluteus larva stage, where *Spu*MHC is expressed in the circumesophageal musculature (Andrikou et al., 2015). In the cephalochordate *Branchiostoma belcheri*, strong *MHC2* (*BbeMHC2*) expression is firstly detected during somitogenesis in the early neurula stage. The larva elongates and *BbeMHC2* begins to be expressed in the notochord as well as in the late neurula stage. *BbeMHC2* remains to be expressed in somites and in the notochord until the first larval stage. Expression ceases in later stages. *BbeMHC1* expression was observed in the somitic mesoderm only (Urano et al., 2003).

In vertebrates, *MHC* is involved in development of skeletal, cardiac, and smooth muscles (McGuigan et al., 2004). Expression domains of the zebrafish *MHC* members *smyhc1* (*DreMHC1*) and *smyhc4* (*DreMHC2*) are found in adaxial cells on both sides of the notochord in the seven somite stage (Bryson-Richardson et al., 2005) when the midbrain forms and the paraxial mesoderm develops (Kimmel et al., 1995). The skeletal musculature of fish consists of a superficial monolayer of so-called slow muscles and deeper layers of

fast muscles. Expression of both *DreMHC1* and *DreMHC2* is active until somite-stage 26 (Bryson-Richardson et al., 2005), when straightening of the posterior trunk is complete and the tail coils ventrally (Kimmel et al., 1995). *DreMHC1* is then expressed in slow muscles and *DreMHC2* in fast muscles only (Bryson-Richardson et al., 2005). Cardiac expression of the chicken (*Gallus gallus*) *MHC* isoforms *AMHC* (*GgaMHC1*) and *VMHC* (*GgaMHC2*) are found during heart development, where *GgaMHC1* is expressed exclusively in the atria and *GgaMHC2* is expressed exclusively in the ventricle (Yutzey et al., 1994). The mouse smooth muscle *MHC* (*MmuMHC*) is expressed in the developing intestine, stomach, uterus, and lungs (Miano et al., 1994).

Data on *MHC* in cnidarian are sparse. In the sea anemone *Nematostella, MHC* (*NveMHC*) transcripts are expressed in the tentacle and retractor muscles of primary polyps. Other stages were not investigated (Renfer et al., 2010).

Taken together, the data currently available suggests an ancestral role of *MHC* in early myogenesis and muscle differentiation in metazoans

Mox gene expression in metazoans

Protostomes (except nematodes) and non-vertebrate deuterostomes commonly possess one *Mox* gene (Chiang et al., 1994; Hinman and Degnan, 2002; Minguillón and Garcia-Fernàndez, 2002; Lowe et al., 2006; Passamaneck et al., 2015; Kozin et al., 2016), whereas vertebrates have two in their genome (Candia et al., 1992; Minguillon and Garcia-Fernandez, 2003). A single *Mox* gene was also found in the hydrozoans *Clytia hemisphaerica* (Chiori et al., 2009) and *Hydra vulgaris* (Reddy et al., 2015). The anthozoan *Nematostella vectensis*, however, has four *Mox* genes that evolved by tandem duplications of the homeobox genes *Mox*, *Hox1*, *Hox2*, and *Otx* (Ryan et al., 2006). This suggests that

the last common cnidarian-bilaterian ancestor possessed one *Mox* gene, and that *Mox* was duplicated in vertebrates.

The lack of *AcaMox1* expression in the gastrula and the expression of *AcaMox1* in the mesodermal bands of *Acanthochitona* is similar to expression patterns of other lophotrochozoans such as the gastropod *Haliotis asinina* (Hinman and Degnan, 2002), the brachiopod *Terebratalia transversa* (Passamaneck et al., 2015), and the polychaete *Alitta virens*, with the latter additionally expressing *Mox* in ectomesodermal cells around the mouth (Kozin et al., 2016). This argues for a conserved expression pattern of *Mox* during mesoderm formation in lophotrochozoans. Furthermore, *AcaMox1* is expressed in the ventrolateral muscle in the late polyplacophoran trochophore larva, which suggests a putative role of *Mox* in molluscan myogenesis. This is corroborated by data on the gastropod *Haliotis asinina*, where *HasMox* is expressed in the developing foot musculature (Hinman and Degnan, 2002). In the polychaete *Alitta virens*, endomesodermal *AviMox* expression is presumably associated with precursor cells of the future oblique muscles of the body wall, while the ectomesodermal *AviMox* expression is associated with precursor cells of the future pharyngeal muscles (Kozin et al., 2016). Data on the brachiopod *Terebratalia transversa* are inconclusive as to whether the *TtrMox* ortholog is expressed in muscle progenitors or in already differentiated muscle tissue (Passamaneck et al., 2015).

In the fruit fly *Drosophila melanogaster,* the *Mox* ortholog *buttonless* (*DmeMox*) is expressed in the dorsal median cells (which derive from the ventral mesoderm), which plays a crucial role in axon guidance in *Drosophila* but not in muscle progenitors or muscular tissue (Chiang et al., 1994). Other ecdysozoans are yet to be tested for *Mox* expression. There is thus a dramatic lack of data in arthropods, and in the second major ecdysozoan group, the nematodes, *Mox* was very likely lost (Ruvkun et al., 1998).

Expression of *gax*, a *Mox* ortholog in the hemichordate *Saccoglossus kowalevskii* (*SkoMox*), was reported in the ventral mesoderm (Lowe et al., 2006). Here, expression is first detected after gastrulation in the paired coelomic cavities of the metasome, i.e. when the mesoderm folds off from the archenteron wall. During further development, *SkoMox* expression in the dorsal region of the metacoel ceases, while ventral expression continues in form of a thin line in the developing metasomal mesoderm where it further extends into the posterior metacoel (Lowe et al., 2006). Data are inconclusive as to whether or not *SkoMox* expression continues during subsequent development of the enteropneust (Lowe et al., 2006).

In the sea urchin *Strongylocentrotus purpuratus*, a *SpuMox* ortholog is not expressed during mesoderm formation but in ectodermal neuronal cells in the region of the larval apical organ (Poustka et al., 2007). Expression disappears in later stages, indicating that *SpuMox* plays a role in early neurogenesis in sea urchins (Poustka et al., 2007). In the ascidian *Ciona intestinalis*, the *Mox* ortholog *Meox* (*CinMox*) is specifically expressed in muscle precursor cells in the early gastrula (Satou and Imai, 2015) and in the cephalochordate *Branchiostoma floridae*, *Mox* (*BbeMox*) is expressed in the paraxial mesoderm during somite formation (Minguillón and Garcia-Fernàndez, 2002). Expression starts from somite 5 onwards, remains active until the somite is formed, and is subsequently downregulated. This pattern is repetitive until all somites have formed (Minguillón and Garcia-Fernàndez, 2002). In the mouse, two *Mox* genes, *MmuMox1 and MmuMox2,* were identified. *MmuMox1* is first expressed in all posterior mesodermal cells after gastrulation. During neurulation, *MmuMox1* is expressed posteriorly in somitic, intermediate, and lateral plate mesoderm (Candia et al., 1992). After somite differentiation, *MmuMox2* expression becomes restricted to the sclerotome and its derivatives (Candia et al., 1992). During further

development, *MmuMox1* expression is in the developing bones, muscles, heart and kidneys (Candia et al., 1992).

Unambiguous *Mox* sequences in the basally branching bilaterian clade Xenacoelomorpha are currently not available.

Fewer data on *Mox* expression are available for cnidarians, where *Mox* is expressed exclusively in the endoderm and not during myogenesis (Chiori et al., 2009; Reddy et al., 2015). In the planula larva of the cnidarian *Nematostella vectensis*, *NveMox* is expressed in the anterior endoderm. This expression pattern remains until the tentacles form and the larva metamorphoses into the polyp (Ryan et al., 2007).

Taken together, the data currently available suggest that *Mox* was recruited into mesoderm formation in the last common bilaterian ancestor and may thus have played an important role in mesoderm evolution (Figure 8). In addition, it appears that *Mox* was simultaneously recruited into myogenesis in Bilateria (with loss of this latter function at least in *Drosophila* and putative loss-of-function in both myogenesis and mesoderm formation in echinoderms; see Fig. 8) but data on the early branching Acoelomorpha are needed to further substantiate this hypothesis.

Hairy and enhancer of split (*HES*) gene expression in metazoans

HES genes are fast evolving genes that have undergone species-specific independent gene duplications (Gazave et al., 2014). The actual number of *HES* sequences varies between one single sequence in the fly *Drosophila* (Carroll et al., 1988), the sea urchin *Strongylocentrotus* (Minokawa et al., 2004), the leech *Helobdella* (Song et al., 2004), and the cnidarian *Hydra* (Münder et al., 2010), two sequences in the snail *Crepidula* (Perry et al., 2015) and the brachiopod *Terebratalia* (Schiemann et al., 2017), six sequences in the

mouse (Kageyama et al., 2007), seven sequences in the sea anemone *Nematostella* (Marlow et al., 2012), eight sequences in the lancelet *Branchiostoma* (Minguillón et al., 2003), and 22 sequences in the zebrafish *Danio* (Gazave et al., 2014). In *Acanthochitona*, seven *HES* sequences were annotated but only two of them, *AcaHESC2* and *AcaHESC7*, yielded results using in situ hybridization.

AcaHESC2 expression is found in the mesodermal bands of the early trochophore larva and in two spot-like domains near the apical organ in the late trochophore larva. We were unable to unequivocally assign the *AcaHESC2* expression domains of the late trochophore larva to distinct (developing) morphological features but their location in the region of the adult polyplacophoran buccal ganglia suggests a function during neurogenesis (cf. Sumner-Rooney & Sigwart 2015). *AcaHESC7* expression is in the trochoblasts, a pattern that so far has not been reported for any lophotrochozoan. *AcaHESC7* expression in the oral ectoderm and around the foregut is similar to the expression patterns of the gastropod *Crepidula fornicata* (Perry et al., 2015). *Crepidula hesA* (*CfoHES1*) expression starts in the early pre-veliger larva and is found in ectodermal cells around the mouth and in ventral neurosensory cells. The expression around the mouth is associated with the formation of the esophagus. During further development, an additional, albeit weak, *CfoHES1* expression domain is present in the anlage of the foot (Perry et al., 2015). *Crepidula hesB* (*CfoHES2*) expression starts asymmetrically in some ectodermal cells in the embryo during gastrulation (Perry et al., 2015). In the gastrula, *CfoHES2* is expressed symmetrically in ectodermal cells flanking the blastopore. This expression domains enlarge and intensify in the pre-veliger larva (Perry et al., 2015). In the brachiopod *Terebratalia*, *TtrHES1* is expressed in the lateral ectoderm of the gastrula where the chaetal sacs will form. In *Terebratalia* larval stages, *TtrHES1* expression was not found (Schiemann et al., 2017). *TtrHES2* is expressed in the mesoderm and in the developing chaete but not during formation of the gut (Schiemann et al., 2017).

In the polychaete annelids *Platynereis* and *Capitella,* 13 and 3 *HES* genes, respectively, are expressed in various body regions, including the growth zone, chaetae, the nervous system, and the digestive tract (Thamm and Seaver, 2008; Gazave et al., 2014). The planarian *HES* gene is expressed in neuronal progenitor cells (Cowles et al., 2013). Accordingly, mollusks share larval *HES* gene expression patterns with other lophotrochozoans during mesoderm and digestive tract formation as well as in neurogenesis (Fig. 9).

The only *Drosophila HES* gene, *hairy* (*DmeHES*), is expressed during segmentation where it acts as a pair-rule gene (Lardelli and Ish-Horowicz, 1993). Expression of *DmeHES* starts at the cellular blastoderm stage, where seven bands and one additional anterior domain of *DmeHES* expression are present. During gastrulation and germ band extension *DmeHES* expression ceases (Carroll et al., 1988). In 28-cell stage embryos of the nematode *Caenorhabditis elegans*, the *HES* gene *ref-1* (*CelHES*) is expressed in descendants of the AB blastomere which contribute to the nervous systems (Lanjuin et al., 2006). After three subsequent cell divisions *CelHES* expression ceases (Lanjuin et al., 2006).

In deuterostomes, expression of the single *HES* gene in the sea urchin *Strongylocentrotus* (*SpuHES*) starts in the blastula stage and appears in three patches in the animal half as well as in a faint crescent-shaped expression in the vegetal half of the embryo (Minokawa et al., 2004). These expression patterns intensify in the late blastula stage prior to archenteron invagination, peak in the gastrula stage, and disappear afterwards. In the late gastrula stage, *SpuHES* expression is restricted to the oral ectoderm and is (weakly) found in the archenteron (Minokawa et al., 2004). In the early pluteus larva, the *SpuHES* expression domains are restricted to the apical organ and the archenteron. Further stages were not investigated (Minokawa et al., 2004).

The amphioxus *Branchiostoma* has eight *HES* genes (*BbeHESA-H*). Four (*BbeHESA-D*) are expressed in the mid-gastrula in the anterior endoderm, in the presumptive neuronal plate, and in the presomitic mesoderm. In the neurula stage, expression is found in the endoderm, in the neural tube, in somites, as well as in the paraxial mesoderm, the foregut, neural plate, and in the notochord (Jiménez-delgado et al., 2006). In larval stages, expression of the *BbeHES* genes is in the dorsal nerve cord, the pharynx, and the digestive tract. *BbeHESE-G* did not yield any expression in the studied stages (Minguillón et al., 2003). In vertebrates (mouse, chicken, and xenopus), *HES* genes play a crucial role during somitogenesis, gut formation, neurogenesis as well as in maintaining of the stem-cell potential, and separation of different brain areas from each other (Palmeirim et al., 1997; Kageyama et al., 2007; Vega-López et al., 2015).

In early embryos of the acoel *Symsagittifera roscoffensis* one *HES* gene (*SroHES*) is expressed in the anterior-median region. In juveniles, *SroHES* is expressed posterior to the statoblast, dorsally in the nerve cords, and mid-ventrally in the brain (Perea-Atienza et al., 2018).

In non-bilaterians, two *HES* genes, namely *NveHES2* and *NveHES3*, are expressed in ectodermal cells of the gastrula in the sea anemone *Nematostella*. While *NveHES2* is widely expressed in the ectoderm, *NveHES3* expression is restricted to the region of the aboral ectoderm. *NveHES2* expression domains are shifted towards the oral ectoderm in late gastrula stages and are restricted to the region around the oral ectoderm in the planula larva. *NveHES3* expression expands to the region of the oral ectoderm and is restricted to oral ecto- and endoderm in the planula larva (Marlow et al., 2012). The single *Hydra HES* gene (*HvuHES*) is expressed during budding at the bud base shortly before separation from the mother animal. Prior to that, no *HvuHES* expression was detected (Münder et al., 2010).

Taken together, *HES* expression domains in lophotrochozoans differ in shape but are confined to similar tissue types (mesoderm, digestive tract, neurons), suggesting a common role of *HES* genes in lophotrochozoan neurogenesis, formation of the digestive tract, and mesoderm development. Additionally, in annelids and brachiopods, HES genes are involved in formation of the chaete (Fig. 9). A broader comparison with other metazoans shows their involvement in separating tissues that are destined to undergo different fates ("territorialisation"), such as segment formation in annelids and arthropods, somitogenesis in chordates, and budding in cnidarians as well as in formation of the digestive tract, and in neurogenesis, demonstrating a wide array of functions of *HES* genes (Fig. 9).

Conclusion

The present study shows that *Mox* and *HES* genes are expressed during mesoderm formation in the mollusk *Acanthochitona*. Expression of *Mox* in the mesodermal bands and in their major derivatives, the muscles, is congruent with the situation in other lophotrochozoans, suggesting a dual function of this gene in the last common bilaterian ancestor with a secondary loss in myogenesis in ecdysozoans and loss in both myogenesis and mesoderm formation in echinoderms, where *Mox* is instead expressed in the ectoderm. Expression of *HES* is during early mesoderm development, neurogenesis and digestive tract formation in a number of bilaterians as well as in ectodermal and endodermal domains in cnidarians, implying either a wide variety of functions already at the dawn of bilaterian evolution or a particularly high degree of functional plasticity (co-option) of *HES* genes that occurred independently along the various bilaterian lineages.

Acknowledgements

I would like to thank to Prof. Thomas Rattei from the division of computational systems biology (CUBE) at the university Vienna for providing access to the multicomputational server. Further, I would like to thank Andreas Hejnol and Pedro Martínez for their engagement in searching for a *Mox* ortholog in acoels. This study was supported by a grant of the Austrian Science Fund (FWF) to Andreas Wanninger (grant number: P29455-B29).

Figures

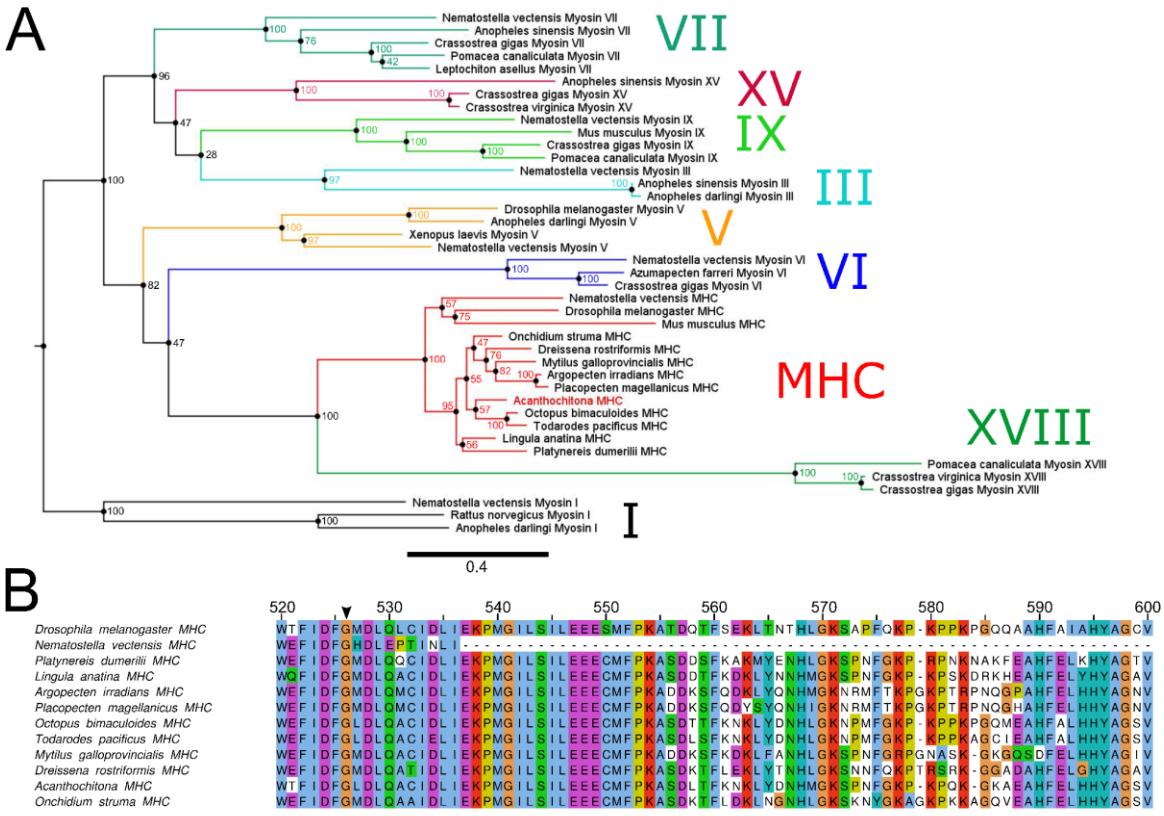

Figure 1. ***Myosin heavy chain*** **phylogeny and alignment.** Nine members of the myosin superfamily that are commonly found in metazoans were included in the analysis. **(A)** Maximum likelihood tree with 100 bootstrap replicates. *AcaMHC* groups with high statistical support with orthologs of other lophotrochozoans. The *Myosin I* clade was used to root the tree. **(B)** Trimmed alignment of the myosin head domain. The *MHC*-specific glycine insertion is indicated by the black arrowhead. Missing data are indicated by dashes. Scalebar indicates substitutions per side.

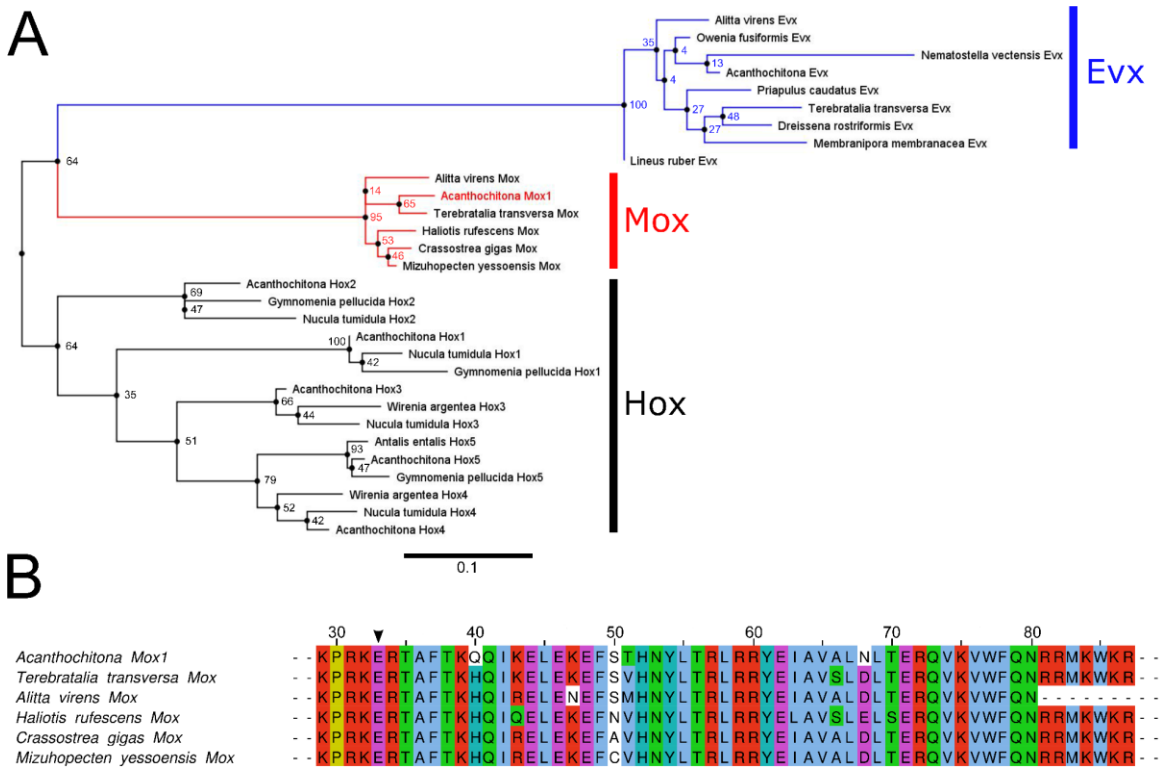

Figure 2. *Mox* phylogeny and alignment. *Evx* was included because it is argued to form the sister group to *Mox* and the *Hox* genes were included because they form the sister group to the *Evx-Mox* clade. **(A)** Maximum likelihood tree with 100 bootstrap replicates. *AcaMox1* groups with high statistical support with orthologs of other lophotrochozoans. The clade of anterior *Hox* genes was used to root the tree. **(B)** Trimmed alignment of the *Mox* homeodomain. The *Mox*-specific glutamic acid residue is indicated by the black arrowhead. Missing data are indicated by dashes. Scalebar indicates substitutions per side.

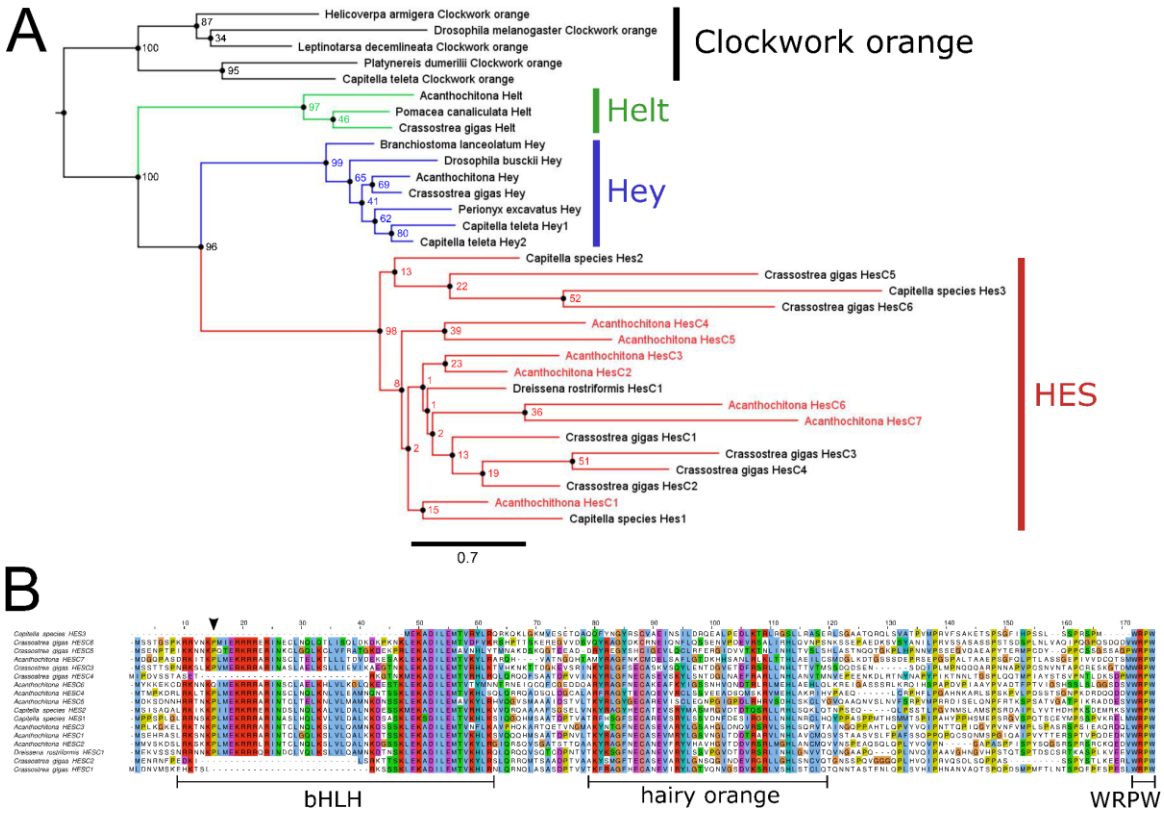

Figure 3. *Hairy and enhancer of split* phylogeny and alignment. *Hey*, *Helt* and *Clockwork orange* were included in the analysis because they are the closest relatives of the *HES* genes. **(A)** Maximum likelihood tree with 100 bootstrap replicates. *AcaHES* groups with high statistical support with orthologs of other lophotrochozoans. The *Clockwork orange* clade was used to root the tree. **(B)** Trimmed alignment of the *HES* gene sequences. *HES* genes consist of two domains, namely a bHLH domain that contains a *HES*-specific proline residue (arrowhead) and a *HES*-specific Hairy orange domain, as well as one *HES*-specific WRPW motif at the C-terminal end. Missing data are indicated by dashes. Scalebar indicates substitutions per side.

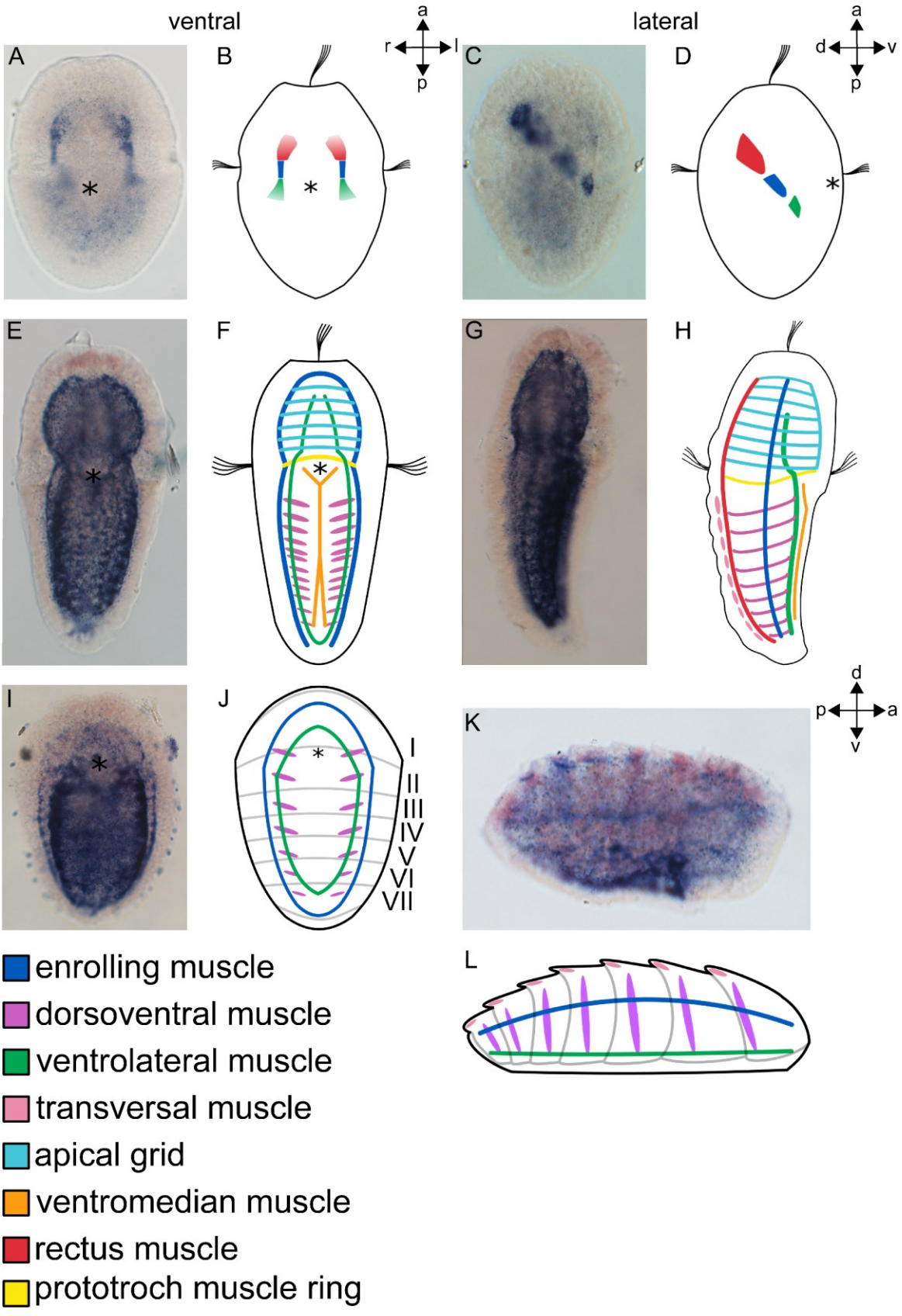

Figure 4. Expression of *AcaMHC* during *Acanthochitona* development. Colour code indicates respective muscle systems. B, D, F, H, J, L are schematic representations of gene

expression signatures of the respective developmental stages. **(A-D)** *AcaMHC* expression in the early trochophore larva **(A)** *AcaMHC* expression in the developing rectus, enrolling, and ventrolateral muscle. **(B)** Ventral view of the developing muscles. **(C)** Lateral right view of the *AcaMHC* expression in developing muscles. **(D)** Lateral right view. **(E-H)** *AcaMHC* expression in the late trochophore larva. **(E)** *AcaMHC* expression is found in all muscles. Dorsally located muscles such as the rectus muscle and the transversal muscles are partially masked by the intense staining of the more ventrally positioned muscles. **(F)** Ventral view. Rectus and transversal muscles are not shown. **(G)** Lateral view showing weak expression in the transversal muscles. **(H)** Lateral right view. **(I-L)** *AcaMHC* expression in the early juvenile. **(I)** *AcaMHC* expression is retained in the enrolling muscle, the ventrolateral muscle, the dorsoventral muscles, and the transversal muscles. **(J)** Ventral view. **(K)** Lateral right view on *AcaMHC* expression. **(L)** Lateral right view. Asterisks mark the mouth. Roman numerals correspond to the juvenile shells. Abbreviations: a = anterior, d = dorsal, l = left, p = posterior, r = right, v = ventral.

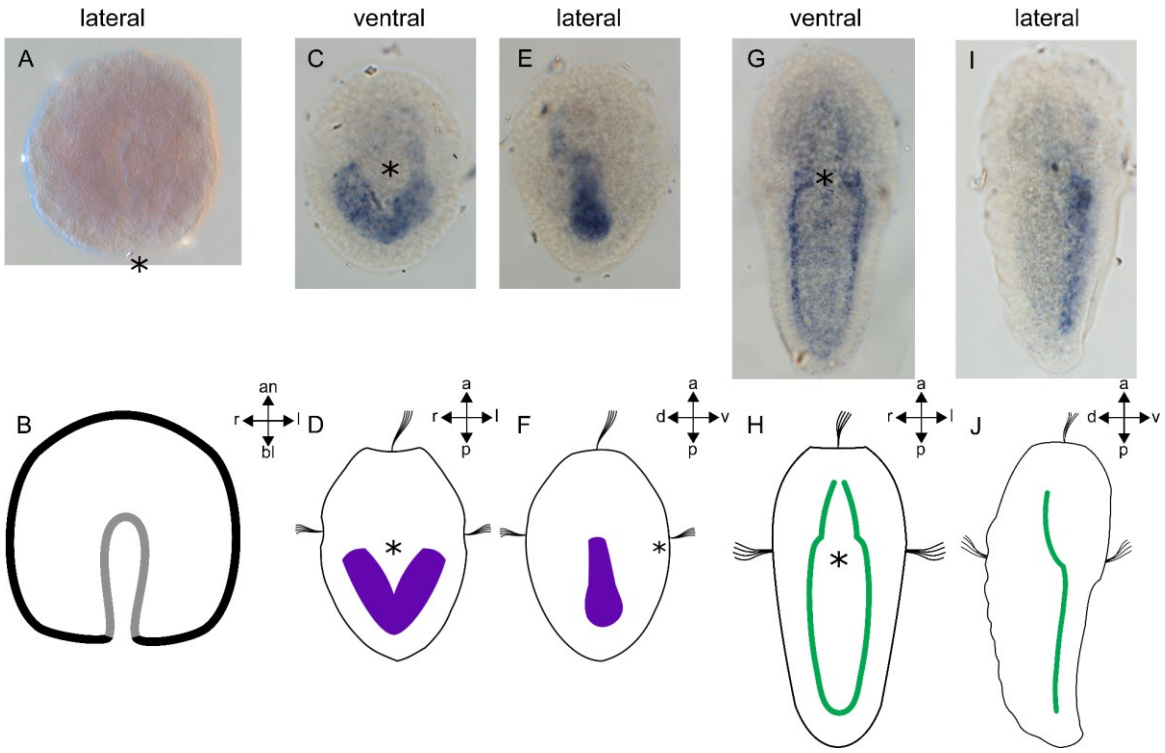

Figure 5. Expression of *AcaMox1* during early mesoderm formation in *Acanthochitona*. B, D, F, H, J, are schematic representations of gene expression signatures of the respective developmental stages. **(A, B)** Expression of *AcaMox1* in the gastrula. **(A)** The gastrula is devoid of *AcaMox1* expression. **(B)** Lateral right view. **(C-F)** *AcaMox1* expression in the early trochophore larva. **(C)** *AcaMox1* is expressed in the mesodermal bands. **(D)** Ventral view. **(E)** Lateral right view on *AcaMox1* expression in the mesodermal bands. **(F)** Lateral right view. **(G-J)** *AcaMox1* expression in the late trochophore larva. **(G)** *AcaMox1* expression in the ventrolateral muscle. **(H)** Ventral view. Ventrolateral muscle in green. **(I)** Lateral right view on *AcaMox1* expression in the ventrolateral muscle. **(J)** Lateral right view. Ventrolateral muscle in green. Asterisks mark the blastopore and the mouth, respectively. Abbreviations: a = anterior, an = animal, bl = blastopore, d = dorsal, l = left, p = posterior, r = right, v = ventral.

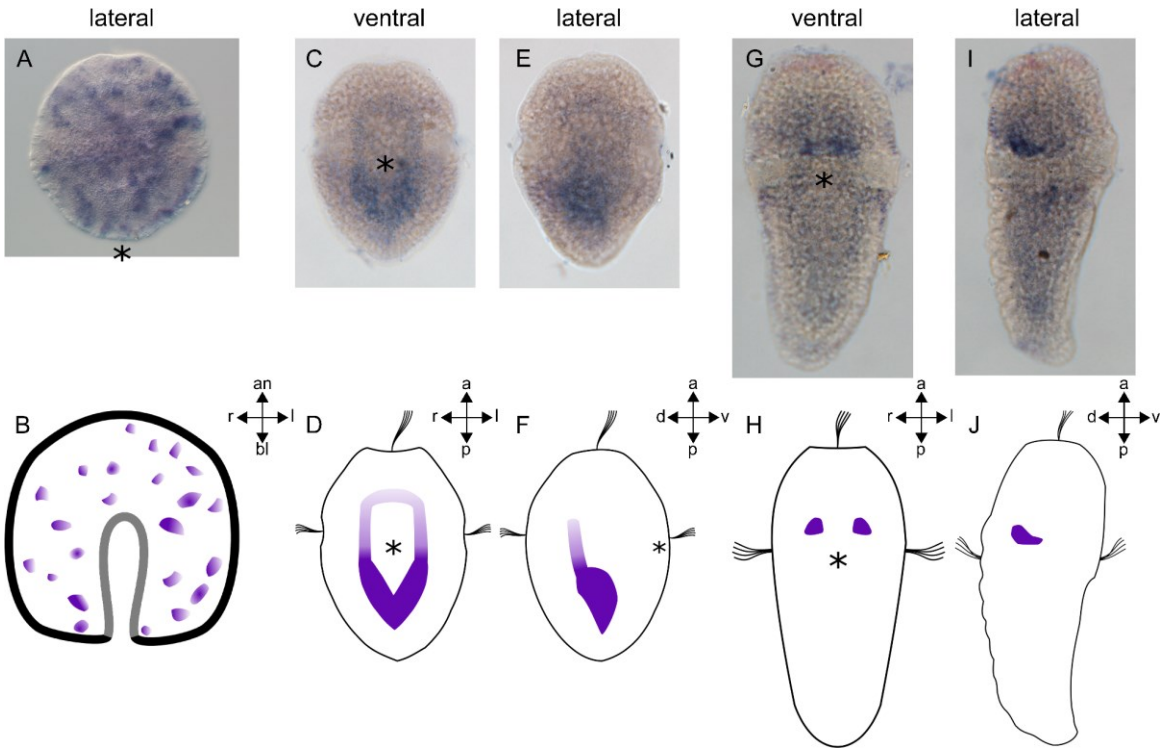

Figure 6. Expression of *AcaHESC2* during early mesoderm formation in *Acanthochitona*. B, D, F, H, J, are schematic representations of gene expression signatures of the respective developmental stages. **(A, B)** Expression of *AcaHESC2* in the gastrula. **(A)** *AcaHESC2* is expressed in ectodermal cells of the gastrula. **(B)** Lateral view **(C-F)** *AcaHESC2* expression in the early trochophore larva. **(C)** *AcaHESC2* is expressed in the mesodermal bands. A weak expression domain extends into the larval episphere. **(D)** Ventral view. **(E)** Lateral right view on *AcaHESC2* expression in the early trochophore larva. A weak expression domain extends into the larval episphere. **(F)** Lateral right view. **(G-J)** *AcaHESC2* expression in the late trochophore larva. **(G)** *AcaHESC2* is expressed in two spot-like domains in the region of the adult buccal ganglia **(H)** Ventral view. **(I)** Lateral view of the *AcaHESC2* expression which shows that the spot-like expression domains are located dorsally. **(J)** Lateral view. Asterisks mark the blastopore and the mouth, respectively. Abbreviations: a = anterior, an = animal, bl = blastopore, d = dorsal, l = left, p = posterior, r = right, v = ventral.

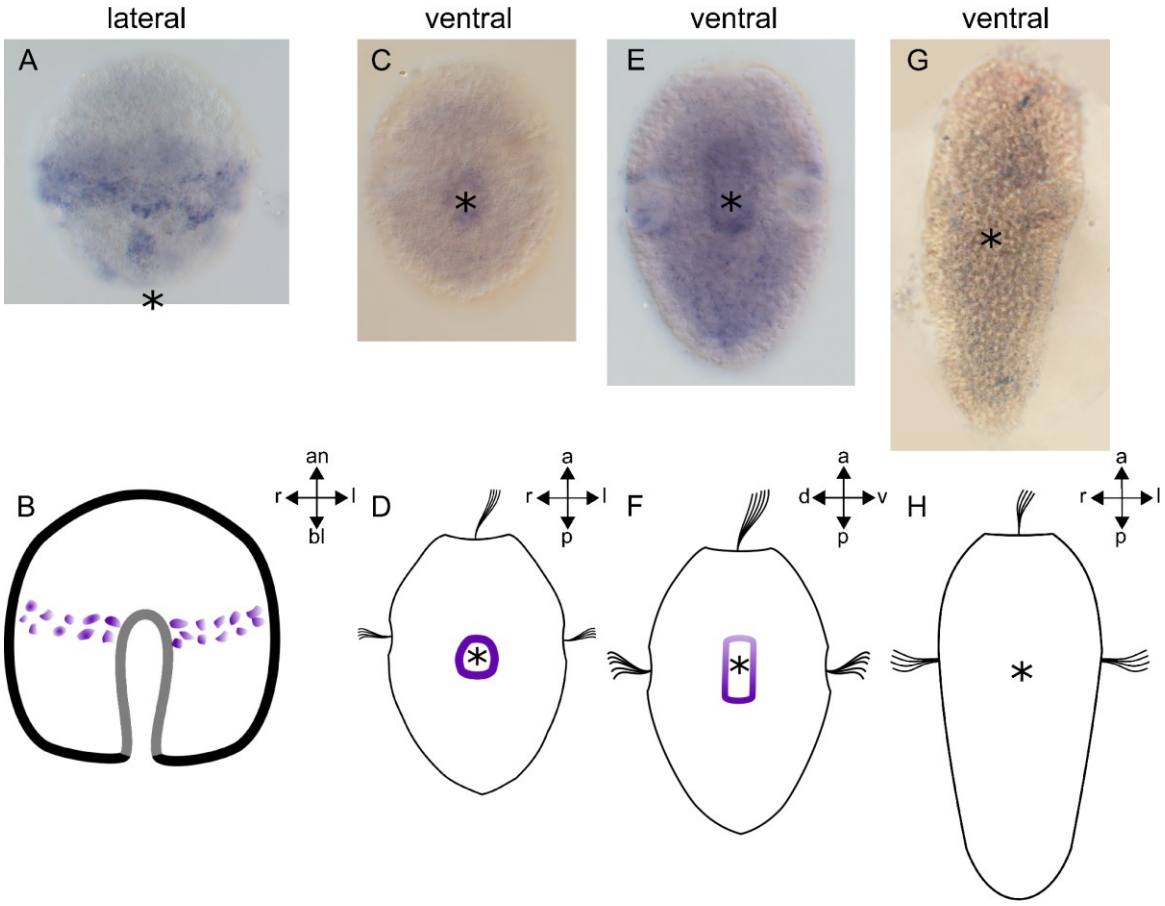

Figure 7. Expression of *AcaHESC7* during development of *Acanthochitona*. B, D, F, H, are schematic representations of gene expression signatures of the respective developmental stages. **(A, B)** Expression of *AcaHESC7* in the gastrula. **(A)** *AcaHESC7* is expressed in the trochoblasts. **(B)** Lateral view. **(C, D)** *AcaHESC7* expression in the early trochophore larva. **(C)** Expression of *AcaHES7* is found in ectodermal cells around the mouth. **(D)** Ventral view. **(E, F)** Expression of *AcaHESC7* in the mid-trochophore larva. **(E)** The expression domain remains around the posterior margin of the mouth and extends anteriorly into the region of the foregut. **(F)** Ventral view. **(G)** Loss of *AcaHESC7* expression in the late trochophore larva. **(H)** Ventral view. Asterisks mark the blastopore and the mouth, respectively. Abbreviations: a = anterior, an = animal, bl = blastopore, d = dorsal, l = left, p = posterior, r = right, v = ventral.

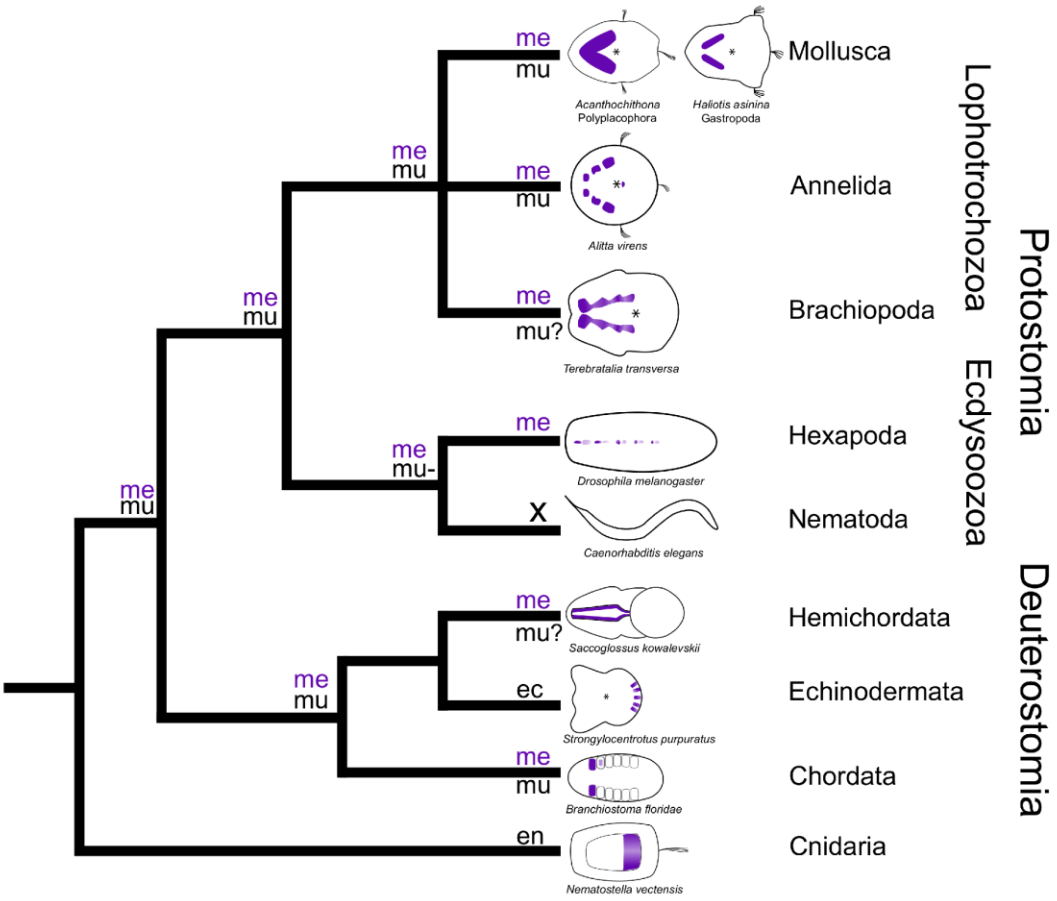

Figure 8. Comparative *Mox* expression in eumetazoans. Mesodermal domains of *Mox* expression in violet in schematic representations. Schemes are in ventral view with anterior to the right. ec = expression in ectoderm, en = expression in endoderm, me = expression in mesoderm, mu = *Mox* expression in developing muscles, mu- = no *Mox* expression in developing muscles, mu? = *Mox* expression in developing muscles not investigated, x = no *Mox* ortholog present. **Lophotrochozoa:** *Mox* is expressed in the mesodermal bands of early lophotrochozoan larvae and additionally in a small pre-oral ectomesodermal domain in *Alitta virens*. *Mox* is also expressed in muscle progenitor cells and/or muscle tissue in later-stage mollusk and annelid larvae. Data on brachiopods are inconclusive. **Ecdysozoa:** The *Mox* ortholog *buttonless* is expressed in dorsal median cells which originate from the mesoderm and play a role in axon guidance but are not associated with myogenesis. Nematodes have no *Mox* ortholog. **Deuterostomia:** *Mox* expression in the mesoderm in

hemichordates and chordates. In the sea urchin, *Mox* is only expressed in neural cells of the larva. *Mox* expression in myogenesis in hemichordates is unknown. In chordates, *Mox* is expressed during somitogenesis in amphioxus and vertebrates. In amphioxus, no *Mox* expression was observed after somitogenesis. In vertebrates, both *Mox* genes are expressed in myogenesis. **Cnidaria:** *Mox* expression is restricted to the endoderm. Parsimony analysis suggests a recruitment of *Mox* in mesoderm formation and myogenesis at the base of bilaterians with a loss in myogenesis in *Drosophila* and a loss in mesoderm formation in echinoderms. Asterisks mark the mouth. Data from Chiang et al., 1994; Ruvkun et al., 1998; Hinman and Degnan, 2002; Minguillón and Garcia-Fernàndez, 2002; Lowe et al., 2006; Poustka et al., 2007; Ryan et al., 2007; Passamaneck et al., 2015; Kozin et al., 2016; present study.

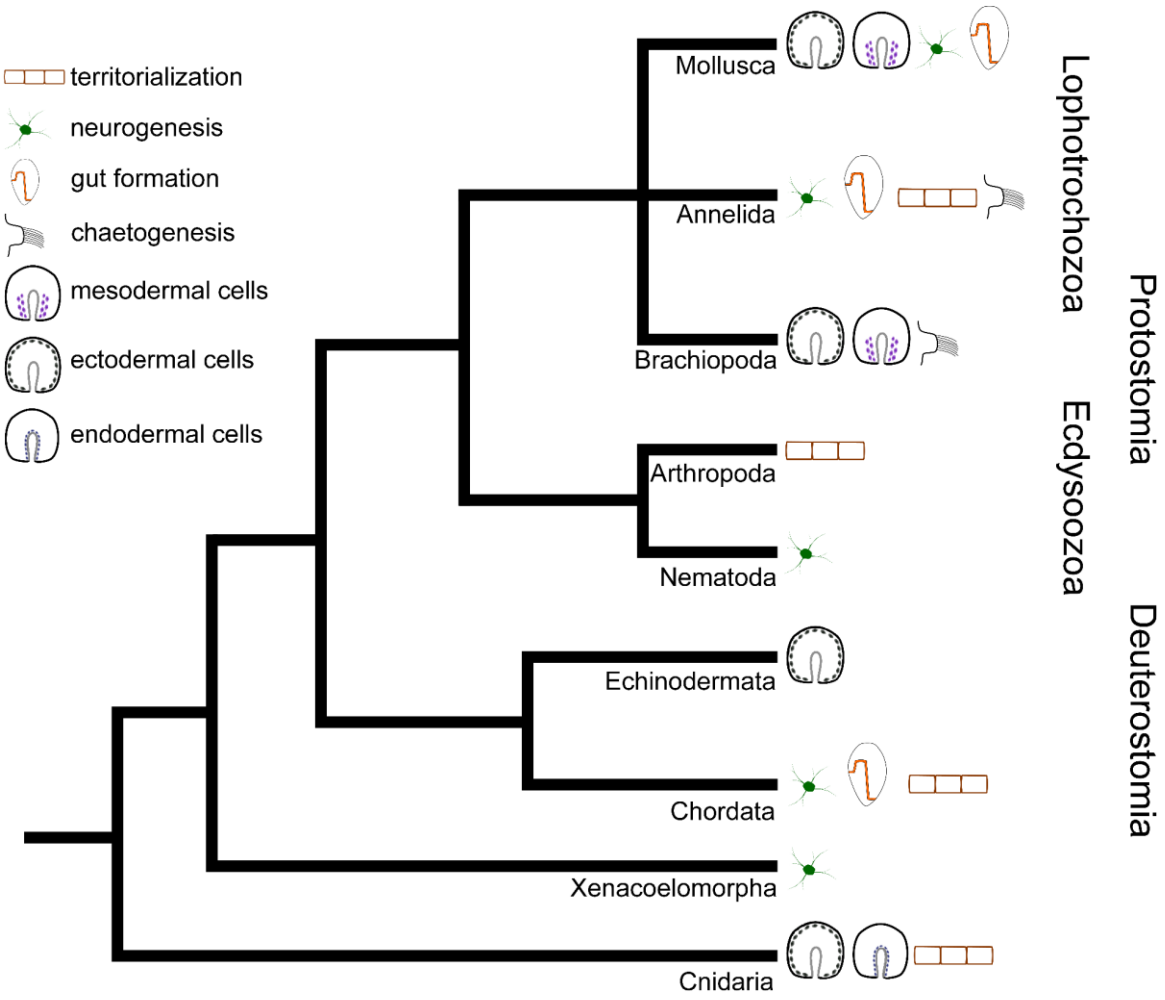

Figure 9. *HES* gene expression in metazoan organogenesis. Lophotrochozoa: (Mollusca) Expression is in ectodermal cells of pre-larval stages and subsequently during mesoderm formation as well as in neurogenesis and development of the digestive tract. **(Annelida)** Expression is during formation of the digestive tract, neurogenesis, segmentation, and chaetogenesis. **(Brachiopoda)** Expression is in the ectoderm of pre-larval stages, during early mesoderm formation and in chaetogenesis. **Ecdysozoa: (Hexapoda)** Expression is during segment formation. **(Nematoda)** Expression is during neurogenesis. **Deuterostomia: (Echinodermata)** Expression is in the larval ectoderm. In the late pluteus larva, *HES* expression is in the region of the apical organ. **(Chordata):** Expression is during neurogenesis, somitogenesis, and in the digestive tract. **(Xenacoelomorpha):** Expression is during neurogenesis. **Cnidaria:** Expression is in the

ectoderm and endoderm of early developmental stages and during budding in hydrozoans. Data from Carroll et al., 1988; Minguillón et al., 2003; Minokawa et al., 2004; Kageyama et al., 2007; Thamm and Seaver, 2008; Münder et al., 2010; Marlow et al., 2012; Gazave et al., 2014; Perry et al., 2015; Schiemann et al., 2017; Perea-Atienza et al., 2018; present study.

Tables

Table 1. Used primes for the gene amplification. F = forward, R = reverse.

Acanthochitona primer		
Gene	Nucleotide sequence	
	F Primer	R Primer
AcaMHC	CTACGACAGGATGTTCAAG	CTTCGTCTGCTTCTCTTG
AcaMox1	GTTACATCACTATCCGCAC	CTCTGAGAAACTGTCATTTGG
AcaHESC1	CGAAGCTTCATCGAAATC	GTCTGTAATGAAGCCAGG
AcaHESC2	GATCTGTGGATATGGTCTC	CTTGGCTCTTCTGAGTTTG
AcaHESC3	CGATCACAGCCATTGAAG	GGTGTAGCACTGATTGATG
AcaHESC4	GAGGTTCACTCCACAATG	CTTGTTGATCACGGTCATC
AcaHESC5	CCATAGACGGACAAACAAG	CAGCTTGCTCTTCAGTTC
AcaHESC6	GGAGCACCTACAAGAAAG	CTCCACACAGAGTCAGAC
AcaHESC7	GGATAAATCGGAGGGTCC	CCTCCACATTGACGTTTG

Table 2. Species list, gene bank accession numbers and protein sequences used for the *Myosin heavy chain* phylogeny.

Gene	Taxon	Species	NCBI access	Original gene ID	New gene ID
Myosin II/heavy chain	Annelida	*Platynereis dumerilii*	AIJ28480.1	myosin heavy chain, partial	*Platynereis dumerilii MHC*
Myosin II/heavy chain	Arthropoda	*Drosophila melanogaster*	NP_523587.4	myosin heavy chain, isoform H	*Drosophila melanogaster MHC*
Myosin II/heavy chain	Brachiopoda	*Lingula anatina*	XP_023932278.1	myosin heavy chain, striated muscle isoform X26	*Lingula anatina MHC*
Myosin II/heavy chain	Cnidaria	*Nematostella vectensis*	EDO44895		*Nematostella vectensis MHC*
Myosin II/heavy chain	Craniata	*Mus musculus*	NP_001159682.1	myosin-15	*Mus musculus MHC*
Myosin II/heavy chain	Mollusca	*Acanthochitona*	acr_tr62264_cds2_fwd		*Acanthochitona MHC*
Myosin II/heavy chain	Mollusca	*Argopecten irradians*	AAC46490.1	myosin heavy chain	*Argopecten irradians MHC*
Myosin II/heavy chain	Mollusca	*Dreissena rostriformis*	Gene.143954		*Dreissena rostriformis MHC*
Myosin II/heavy chain	Mollusca	*Mytilus galloprovincialis*	CAB64662.1	myosin heavy chain, partial	*Mytilus galloprovincialis MHC*
Myosin II/heavy chain	Mollusca	*Octopus bimaculoides*	CDG41623.1	myosin heavy chain isoform A	*Octopus bimaculoides MHC*
Myosin II/heavy chain	Mollusca	*Onchidium struma*	AOR06339.1	myosin heavy chain	*Onchidium struma MHC*
Myosin II/heavy chain	Mollusca	*Placopecten magellanicus*	AAB03661.1	myosin heavy chain	*Placopecten magellanicus MHC*
Myosin II/heavy chain	Mollusca	*Todarodes pacificus*	ADU19853.1	myosin heavy chain	*Todarodes pacificus MHC*
Myosin I	Arthropoda	*Anopheles darlingi*	ETN59929.1	myosin i	*Anopheles darlingi Myosin I*
Myosin I	Cnidaria	*Nematostella vectensis*	EDO35007		*Nematostella vectensis Myosin I*
Myosin I	Craniata	*Rattus norvegicus*	CAA50871.1	myosin I	*Rattus norvegicus Myosin I*
Myosin III	Arthropoda	*Anopheles sinensis*	KFB46475.1	myosin iii	*Anopheles sinensis Myosin III*
Myosin III	Arthropoda	*Anopheles darlingi*	ETN67236.1	myosin III	*Anopheles darlingi Myosin III*
Myosin III	Cnidaria	*Nematostella vectensis*	EDO45746		*Nematostella vectensis Myosin III*
Myosin V	Arthropoda	*Anopheles darlingi*	ETN63934.1	myosin v	*Anopheles darlingi Myosin V*
Myosin V	Arthropoda	*Drosophila melanogaster*	AAC99496.1	myosin V	*Drosophila melanogaster Myosin V*
Myosin V	Cnidaria	*Nematostella vectensis*	EDO41819		*Nematostella vectensis Myosin V*
Myosin VI	Cnidaria	*Nematostella vectensis*	EDO36037		*Nematostella vectensis Myosin VI*
Myosin V	Craniata	*Xenopus laevis*	AFU81219.2	myosin V	*Xenopus laevis Myosin V*
Myosin VI	Mollusca	*Azumapecten farreri*	AAY63881.1	myosin VI, partial	*Azumapecten farreri VI*
Myosin VI	Mollusca	*Crassostrea gigas*	EKC25309.1	Myosin-VI	*Crassostrea gigas Myosin VI*
Myosin VII	Arthropoda	*Anopheles sinensis*	KFB45621.1	myosin vii	*Anopheles sinensis Myosin VII*
Myosin VII	Cnidaria	*Nematostella vectensis*	EDO45563		*Nematostella vectensis Myosin VII*
Myosin VII	Mollusca	*Crassostrea gigas*	EKC28928.1	Myosin-VIIa	*Crassostrea gigas Myosin VII*
Myosin VII	Mollusca	*Leptochiton asellus*	ASM47588.1	myosin VIIa	*Leptochiton asellus Myosin VII*
Myosin VII	Mollusca	*Pomacea canaliculata*	XP_025078688.1	myosin-VIIa-like isoform X1	*Pomacea canaliculata Myosin VII*
Myosin IX	Cnidaria	*Nematostella vectensis*	EDO38834		*Nematostella vectensis Myosin IX*
Myosin IX	Craniata	*Mus musculus*	AAI38455.1	Myosin Ixb	*Mus musculus Myosin IX*
Myosin IX	Mollusca	*Crassostrea gigas*	XP_011417195.1	PREDICTED: unconventional myosin-IXa isoform X4	*Crassostrea gigas Myosin IX*
Myosin IX	Mollusca	*Pomacea canaliculata*	XP_025078508.1	unconventional myosin-IXa-like isoform X12	*Pomacea canaliculata Myosin IX*
Myosin XV	Arthropoda	*Anopheles sinensis*	KFB48001.1	myosin xv	*Anopheles sinensis Myosin XV*
Myosin XV	Mollusca	*Crassostrea gigas*	EKC41639.1	Myosin-XV	*Crassostrea gigas Myosin XV*
Myosin XV	Mollusca	*Crassostrea virginica*	XP_022313584.1	unconventional myosin-XV-like isoform X12	*Crassostrea virginica Myosin XV*
Myosin XVIII	Mollusca	*Crassostrea gigas*	XP_011450865.1	PREDICTED: unconventional myosin-XVIIIa isoform X1	*Crassostrea gigas Myosin XVIII*
Myosin XVIII	Mollusca	*Crassostrea virginica*	XP_022343135.1	unconventional myosin-XVIIIa-like isoform X1	*Crassostrea virginica Myosin XVIII*
Myosin XVIII	Mollusca	*Pomacea canaliculata*	XP_025090257.1	unconventional myosin-XVIIIa-like isoform X1	*Pomacea canaliculata Myosin XVIII*

Table 3. Species list, gene bank accession numbers and protein sequences used for the *Mox* phylogeny.

Gene		Species	NCBI access	Original gene ID	New gene ID
Evx	Annelida	*Alitta virens*	AOS87315.1	even-skipped	*Alitta virens Evx*
Evx	Annelida	*Lineus ruber*	AMR72025.1	evx	*Lineus ruber Evx*
Evx	Annelida	*Owenia fusiformis*	AMY99557.1	evx	*Owenia fusiformis Evx*
Evx	Brachiopoda	*Terebratalia transversa*	AHY88463.1	evx	*Terebratalia transversa Evx*
Evx	Bryozoa	*Membranipora membranacea*	ARJ36942.1	even-skipped	*Membranipora membranacea Evx*
Evx	Cnidaria	*Nematostella vectensis*	SJX71987.1	Homeobox gene Evx, partial	*Nematostella vectensis Evx*
Evx	Mollusca	*Acanthochitona*		acr_tr120485_cds1_fwd	*Acanthochitona Evx*
Evx	Mollusca	*Dreissena rostriformis*		Gene.109262	*Dreissena rostriformis Evx*
Evx	Priapulida	*Priapulus caudatus*	AKU77019.1	evx	*Priapulus caudatus Evx*
Mox	Annelida	*Alitta virens*	AOS87316.1	mox, partial	*Alitta virens Mox*
Mox	Brachiopoda	*Terebratalia transversa*	AJV21315.1	mesoderm homeobox	*Terebratalia transversa Mox*
Mox	Mollusca	*Acanthochitona*		acr_tr238840_cds2_rev	*Acanthochitona Mox1*
Mox	Mollusca	*Crassostrea gigas*	EKC25209	Homeobox protein MOX-2	*Crassostrea gigas Mox*
Mox	Mollusca	*Haliotis rufescens*	CAA53027.1	Hrox1	*Haliotis rufescens Mox*
Mox	Mollusca	*Mizuhopecten yessoensis*	KP79_PYT03723	Homeobox protein MOX-2	*Mizuhopecten yessoensis Mox*
Hox1	Mollusca	*Acanthochitona*	APD15641.1	homeobox hox 1	*Acanthochitona Hox1*
Hox1	Mollusca	*Gymnomenia pellucida*	APD15663.1	homeobox hox 1	*Gymnomenia pellucida Hox1*
Hox1	Mollusca	*Nucula tumidula*	APD15698.1	homeobox hox 1	*Nucula tumidula Hox1*
Hox2	Mollusca	*Acanthochitona*	APD15642.1	homeobox hox 2	*Acanthochitona Hox2*
Hox2	Mollusca	*Gymnomenia pellucida*	APD15664.1	homeobox hox 2	*Gymnomenia pellucida Hox2*
Hox2	Mollusca	*Nucula tumidula*	APD15699.1	homeobox hox 2	*Nucula tumidula Hox2*
Hox3	Mollusca	*Acanthochitona*	APD15643.1	homeobox hox 3	*Acanthochitona Hox3*
Hox3	Mollusca	*Nucula tumidula*	APD15700.1	homeobox hox 3	*Nucula tumidula Hox3*
Hox3	Mollusca	*Wirenia argentea*	APD15711.1	homeobox hox 3	*Wirenia argentea Hox3*
Hox4	Mollusca	*Acanthochitona*	APD15644.1	homeobox hox 4	*Acanthochitona Hox4*
Hox4	Mollusca	*Nucula tumidula*	APD15701.1	homeobox hox 4	*Nucula tumidula Hox4*
Hox4	Mollusca	*Wirenia argentea*	APD15712.1	homeobox hox 4	*Wirenia argentea Hox4*
Hox5	Mollusca	*Acanthochitona*	APD15645.1	homeobox hox 5	*Acanthochitona Hox5*
Hox5	Mollusca	*Antalis entalis*	APD15655.1	homeobox hox 5	*Antalis entalis Hox5*
Hox5	Mollusca	*Gymnomenia pellucida*	APD15667.1	homeobox hox 5	*Gymnomenia pellucida Hox5*

Table 4. Species list, gene bank accession numbers and protein sequences used for the *hairy and enhancer of split* phylogeny.

Gene	Taxon	Species	NCBI access	Original gene ID	New gene ID
HES	Annelida	*Capitella sp.*	DQ384620	hairy protein mRNA, complete cds.	*Capitella species HES1*
HES	Annelida	*Capitella sp.*	EU706455.1	HES2 (hes2) mRNA, partial cds.	*Capitella species HES2*
HES	Annelida	*Capitella sp.*	EU706456.1	HES3 (hes3) mRNA, partial cds.	*Capitella species HES3*
HES	Mollusca	*Acanthochitona*		acr_tr122850_cds1_fwd	*Acanthochitona HESC1*
HES	Mollusca	*Acanthochitona*		acr_tr237216_cds4_rev	*Acanthochitona HESC2*
HES	Mollusca	*Acanthochitona*		acr_tr288909_cds2_rev	*Acanthochitona HESC3*
HES	Mollusca	*Acanthochitona*		acr_tr146030_cds2_rev	*Acanthochitona HESC4*
HES	Mollusca	*Acanthochitona*		acr_tr264437_cds1_fwd	*Acanthochitona HESC5*
HES	Mollusca	*Acanthochitona*		acr_tr284209_cds1_fwd	*Acanthochitona HESC6*
HES	Mollusca	*Acanthochitona*		acr_tr239548_cds1_fwd	*Acanthochitona HESC7*
HES	Mollusca	*Dreissena rostriformis*		Gene.33105	*Dreissena rostriformis HESC1*
HES	Mollusca	*Crassostrea gigas*		EKC30677	*Crassostrea gigas HESC1*
HES	Mollusca	*Crassostrea gigas*		EKC30678	*Crassostrea gigas HESC2*
HES	Mollusca	*Crassostrea gigas*		EKC23398	*Crassostrea gigas HESC3*
HES	Mollusca	*Crassostrea gigas*		EKC23396	*Crassostrea gigas HESC4*
HES	Mollusca	*Crassostrea gigas*		EKC43182	*Crassostrea gigas HESC5*
HES	Mollusca	*Crassostrea gigas*		EKC30676	*Crassostrea gigas HESC6*
Hey	Annelida	*Capitella teleta*		CapteP228069	*Capitella teleta Hey1*
Hey	Annelida	*Capitella teleta*		CapteP182542	*Capitella teleta Hey2*
Hey	Annelida	*Perionyx excavatus*	ASQ42633.1	HEY, partial	*Perionyx excavatus Hey*
Hey	Arthropoda	*Drosophila busckii*	ALC41030.1	Hey	*Drosophila busckii Hey*
Hey	Cephalochordata	*Branchiostoma lanceolatum*	AWV91612.1	hey	*Branchiostoma lanceolatum Hey*
Hey	Mollusca	*Acanthochitona*		acr_tr163747_cds1_fwd	*Acanthochitona Hey*
Hey	Mollusca	*Crassostrea gigas*		EKC34248	*Crassostrea gigas Hey*
Helt	Mollusca	*Acanthochitona*		acr_tr149761_cds1_fwd	*Acanthochitona Helt*
Helt	Mollusca	*Crassostrea gigas*		EKC36048	*Crassostrea gigas Helt*
Helt	Mollusca	*Pomacea canaliculata*	XP_025115546.1	HES-related protein helt-like	*Pomacea canaliculata Helt*
Clockwork orange	Annelida	*Capitella teleta*		CapteP196737	*Capitella teleta Clockwork orange*
Clockwork orange	Annelida	*Platynereis dumerilii*	AGS55449	hairy enhancer of split related	*Platynereis dumerilii Clockwork orange*
Clockwork orange	Arthropoda	*Drosophila melanogaster*	NP_001247025.1	clockwork orange, isoform C	*Drosophila melanogaster Clockwork orange*
Clockwork orange	Arthropoda	*Helicoverpa armigera*	ARQ15181.1	clockwork orange	*Helicoverpa armigera Clockwork orange*
Clockwork orange	Arthropoda	*Leptinotarsa decemlineata*	AKG92774.1	clockwork orange	*Leptinotarsa decemlineata Clockwork orange*

References

Abascal, F., Zardoya, R., Posada, D., 2005. ProtTest: Selection of best-fit models of protein evolution. *Bioinformatics* 21, 2104–2105.

Akaike, H., 1973. Information theory and an extension of the maximum likelihood principle. In B. N. Petrov, & F. Csaki (Eds.), *Proceedings of the 2nd International Symposium on Information Theory*, 267-281.

Altschul, S.F., Gish, W., Miller, W., Myers, E.W., Lipman, D.J., 1990. Basic local alignment search tool. *J. Mol. Biol.* 215, 403–410.

Anderson, D.T., 1973. Embryology and Phylogeny in Annelids and Arthropods. *Pergamon Press*.

Andrikou, C., Pai, C.Y., Su, Y.H., Arnone, M.I., 2015. Logics and properties of a genetic regulatory program that drives embryonic muscle development in an echinoderm. *Elife* 4, 1–22.

Artimo, P., Jonnalagedda, M., Arnold, K., Baratin, D., Csardi, G., de Castro, E., Duvaud, S., Flegel, V., Fortier, A., Gasteiger, E., Grosdidier, A., Hernandez, C., Ioannidis, V., Kuznetsov, D., Liechti, R., Moretti, S., Mostaguir, K., Redaschi, N., Rossier, G., Xenarios, I., Stockinger, H., 2012. ExPASy: SIB bioinformatics resource portal. *Nucleic Acids Res.* 40, W597-W603.

Banerjee-Basu, S., Baxevanis, A.D., 2001. Molecular evolution of the homeodomain family of transcription factors. *Nucleic Acids Res.* 29, 3258–3269.

Bejsovec, A., Anderson, P., 1988. Myosin heavy-chain mutations that disrupt *Caenorhabditis elegans* thick filament assembly. *Genes Dev.* 2, 1307–1317.

Boyer, B.C., Henry, J.Q., Martindale, M.Q., 1996. Dual origins of mesoderm in a basal spiralian: Cell lineage analyses in the polyclad turbellarian *Hoploplana inquilina*. *Dev. Biol.* 179, 329–338.

Brunet, T., Fischer, A.H.L., Steinmetz, P.R.H., Lauri, A., Bertucci, P., Arendt, D., 2016. The evolutionary origin of bilaterian smooth and striated myocytes. *Elife* 5, 1–24.

Bryson-Richardson, R.J., Daggett, D.F., Cortes, F., Neyt, C., Keenan, D.G., Currie, P.D., 2005. Myosin heavy chain expression in zebrafish and slow muscle composition. *Dev. Dyn.* 233, 1018–1022.

Burton, P.M., 2008. Insights from diploblasts; the evolution of mesoderm and muscle. *J. Exp. Zool. B. Mol. Dev. Evol.* 310, 5–14.

Candia, A.F., Hu, J., Crosby, J., Lalley, P.A., Noden, D., Nadeau, J.H., Wright, C. V, 1992. *Mox-1* and *Mox-2* define a novel homeobox gene subfamily and are differentially expressed during early mesodermal patterning in mouse embryos. *Development* 116, 1123–36.

Cardona, A., Fernández, J., Solana, J., Romero, R., 2005a. An in situ hybridization protocol for planarian embryos: Monitoring myosin heavy chain gene expression. *Dev. Genes Evol.* 215, 482–488.

Cardona, A., Hartenstein, V., Romero, R., 2005b. The embryonic development of the triclad *Schmidtea polychroa*. *Dev. Genes Evol.* 215, 109–131.

Carroll, S.B., Laughon, A., Thalley, B.S., 1988. Expression, function, and regulation of the hairy segmentation protein in the *Drosophila* embryo. *Genes Dev.* 2, 883–890.

Chiang, C., Patel, N.H., Young, K.E., Beachy, P.A., 1994. The novel homeodomain gene *buttonless* specifies differentiation and axonal guidance functions of *Drosophila* dorsal median cells. *Development* 120, 3581–93.

Chiodin, M., Børve, A., Berezikov, E., Ladurner, P., Martinez, P., Hejnol, A., 2013. Mesodermal gene expression in the acoel *Isodiametra pulchra* indicates a low number of mesodermal cell types and the endomesodermal origin of the gonads. *PLoS One* 8, e55499

Chiori, R., Jager, M., Denker, E., Wincker, P., Da Silva, C., Le Guyader, H., Manuel, M., Quéinnec, E., 2009. Are hox genes ancestrally involved in axial patterning? Evidence from the hydrozoan *Clytia hemisphaerica* (cnidaria). *PLoS One* 4, e4231

Conklin, E.G., 1897. The embryology of *Crepidula*. *J. Morphol*. 8, 1-205

Cowles, M.W., Brown, D.D.R., Nisperos, S. V, Stanley, B.N., Pearson, B.J., Zayas, R.M., 2013. Genome-wide analysis of the bHLH gene family in planarians identifies factors required for adult neurogenesis and neuronal regeneration. *Development* 140, 4691–4702.

Criscuolo, A., Gribaldo, S., 2010. BMGE (block mapping and gathering with entropy): A new software for selection of phylogenetic informative regions from multiple sequence alignments. *BMC Evol. Biol*. 10, 1–21.

Darriba, D., Taboada, G.L., Doallo, R., Posada, D., 2017. ProtTest 3: fast selection of best-fit models of protein evolution. *Bioinformatics* 27, 1164–1165.

De Oliveira, A.L., Wollesen, T., Kristof, A., Scherholz, M., Redl, E., Todt, C., Bleidorn, C., Wanninger, A., 2016. Comparative transcriptomics enlarges the toolkit of known developmental genes in mollusks. *BMC Genomics* 17, 1–23.

Eddy, S.R., 1995. Multiple alignment using hidden markov models. *ISMB-95*, 114-120

Fischer, A.H.L., Arendt, D., 2013. Mesoteloblast-like mesodermal stem cells in the polychaete annelid *Platynereis dumerilii* (Nereididae). *J. Exp. Zool*. 1–11.

Fu, L., Niu, B., Zhu, Z., Wu, S., Li, W., 2012. CD-HIT: Accelerated for clustering the next-generation sequencing data. *Bioinformatics* 28, 3150–3152.

Gazave, E., Guillou, A., Balavoine, G., 2014. History of a prolific family: The *Hes/Hey*-related genes of the annelid *Platynereis*. *Evodevo* 5, 1–33.

Guindon, S., Gascuel, O., 2003. A simple, fast, and accurate algorithm to estimate large phylogenies by maximum likelihood. *Syst. Biol.* 52, 696–704.

Hartenstein, V., Chipman, A.D., 2015. Hexapoda: A *Drosophila*'s view of development, in: Wanninger, A. (Ed.), Evolutionary Developmental Biology of Invertebrates 5: Ecdysozoa III: Hexapoda. *Springer Verlag*, Vienna, 1–91.

Hinman, V.F., Degnan, B.M., 2002. *Mox* homeobox expression in muscle lineage of the gastropod *Haliotis asinina*: Evidence for a conserved role in bilaterian myogenesis. *Dev. Genes Evol.* 212, 141–144.

Holmes, S.J., 1900. Development *Planorbis*. *J. Morphol.* 16, 1–458.

Iso, T., Kedes, L., Hamamori, Y., 2003. HES and HERP families: Multiple effectors of the Notch signaling pathway. *J. Cell. Physiol.* 194, 237–255.

Jiménez-delgado, S., Crespo, M., Permanyer, J., Garcia-fernàndez, J., Manzanares, M., 2006. Evolutionary genomics of the recently duplicated amphioxus Hairy genes. *Int. J. Biol. Sci*. 2, 66–72.

Kageyama, R., Ohtsuka, T., Kobayashi, T., 2007. The Hes gene family: repressors and oscillators that orchestrate embryogenesis. *Development* 134, 1243–1251.

Katoh, K., Misawa, K., Kuma, K., Miyata, T., 2002. MAFFT: a novel method for rapid multiple sequence alignment based on fast Fourier transform. *Nucleic Acids Res*. 30, 3059–3066.

Kibbe, W.A., 2007. OligoCalc: an online oligonucleotide properties calculator. *Nucleic Acids Res.* 35, W43-W46.

Kimmel, C.B., Ballard, W.W., Kimmel, S.R., Ullmann, B., Schilling, T.F., 1995. Stages of embryonic development of the zebrafish. *Dev. Dyn.* 203, 253–310.

Kozin, V. V., Filimonova, D.A., Kupriashova, E.E., Kostyuchenko, R.P., 2016. Mesoderm patterning and morphogenesis in the polychaete *Alitta virens* (Spiralia, Annelida): Expression of mesodermal markers *Twist*, *Mox*, *Evx* and functional role for MAP kinase signaling. *Mech. Dev*. 140, 1–11.

Lanjuin, A., Claggett, J., Shibuya, M., Hunter, C., Sengupta, P., 2006. Regulation of neuronal lineage decisions by the HES-related bHLH protein REF-1. *Dev. Biol.* 290, 139-151

Lardelli, M., Ish-Horowicz, D., 1993. *Drosophila hairy* pair-rule gene regulates embryonic patterning outside its apparent stripe domains. *Development* 118, 255–266.

Larsson, A., 2014. AliView: A fast and lightweight alignment viewer and editor for large datasets. *Bioinformatics* 30, 3276–3278.

Le, S.Q., Gascuel, O., 2008. An improved general amino acid replacement matrix. *Mol. Cell. Biol*. 25, 1307–1320.

Li, W., Godzik, A., 2006. Cd-hit: A fast program for clustering and comparing large sets of protein or nucleotide sequences. *Bioinformatics* 22, 1658–1659.

Lowe, C.J., Terasaki, M., Wu, M., Freeman, R.M., Runft, L., Kwan, K., Haigo, S., Aronowicz, J., Lander, E., Gruber, C., Smith, M., Kirschner, M., Gerhart, J., 2006. Dorsoventral patterning in hemichordates: Insights into early chordate evolution. *PLoS Biol.* 4, 1603–1619.

Mackenzie, J.M., Schachat, F., Epstein, H.F., 1978. Immunocytochemical localization of two myosins within the same muscle cells in *Caenorhabditis elegans*. *Cell* 15, 413–419.

Marlow, H., Roettinger, E., Boekhout, M., Martindale, M.Q., 2012. Functional roles of Notch signaling in the cnidarian *Nematostella vectensis*. *Dev. Biol.* 362, 295–308.

Martindale, M.Q., 2004. Investigating the origins of triploblasty: 'mesodermal' gene expression in a diploblastic animal, the sea anemone *Nematostella vectensis* (phylum, Cnidaria; class, Anthozoa). *Development* 131, 2463–2474.

McGuigan, K., Phillips, P.C., Postlethwait, J.H., 2004. Evolution of sarcomeric myosin heavy chain genes: Evidence from fish. *Mol. Biol. Evol*. 21, 1042–1056.

Miano, J.M., Cserjesi, P., Ligon, K.L., Periasamy, M., Olson, E.N., 1994. Smooth muscle myosin heavy chain exclusively marks the smooth muscle lineage during mouse embryogenesis. *Circ. Res.* 75, 803–812.

Minguillon, C., Garcia-Fernandez, J., 2003. Genesis and evolution of the *Evx* and *Mox* genes and the extended Hox and ParaHox gene clusters. *Genome Biol.* 4, R12.

Minguillón, C., Garcia-Fernàndez, J., 2002. The single amphioxus *Mox* gene: Insights into the functional evolution of *Mox* genes, somites, and the asymmetry of amphioxus somitogenesis. *Dev. Biol.* 246, 455–465.

Minguillón, C., Jiménez-delgado, S., Panopoulou, G., Garcia-fernàndez, J., 2003. The amphioxus Hairy family: Differential fate after duplication. *Development* 130, 5903–5914.

Minokawa, T., Rast, J.P., Arenas-mena, C., Franco, C.B., Davidson, E.H., 2004. Expression patterns of four different regulatory genes that function during sea urchin development. *Gene Expr. Patterns* 4, 449–456.

Münder, S., Käsbauer, T., Prexl, A., Aufschnaiter, R., Zhang, X., Towb, P., Böttger, A., 2010. Notch signalling defines critical boundary during budding in *Hydra*. *Dev. Biol*. 344, 331–345.

Palmeirim, I., Henrique, D., Ish-Horowicz, D., Pourquié, O., 1997. Avian *hairy* gene expression identifies a molecular clock linked to vertebrate segmentation and somitogenesis. *Cell* 91, 639–648.

Passamaneck, Y.J., Hejnol, A., Martindale, M.Q., 2015. Mesodermal gene expression during the embryonic and larval development of the articulate brachiopod *Terebratalia transversa*. *Evodevo* 6, 1–21.

Perea-Atienza, E., Sprecher, S.G., Martínez, P., 2018. Characterization of the bHLH family of transcriptional regulators in the acoel *S. roscoffensis* and their putative role in neurogenesis. *Evodevo* 9, 1-16.

Perry, K.J., Lyons, D.C., Truchado-Garcia, M., Fischer, A.H.L., Helfrich, L.W., Johansson, K.B., Diamond, J.C., Grande, C., Henry, J.Q., 2015. Deployment of regulatory

genes during gastrulation and germ layer specification in a model spiralian mollusc *Crepidula*. *Dev. Dyn.* 244, 1215–1248.

Pfeifer, K., Schaub, C., Domsch, K., Dorresteijn, A., Wolfstetter, G., 2014. Maternal inheritance of *Twist* and Analysis of MAPK activation in embryos of the polychaete annelid *Platynereis dumerilii*. *PLoS One* 9, 1–9.

Pollard, S.L., Holland, P.W.H., 2000. Evidence for 14 homeobox gene clusters in human genome ancestry. *Curr. Biol*. 10, 1059–1062.

Poustka, A.J., Kühn, A., Groth, D., Weise, V., Yaguchi, S., Burke, R.D., Herwig, R., Lehrach, H., Panopoulou, G., 2007. A global view of gene expression in lithium and zinc treated sea urchin embryos: New components of gene regulatory networks. *Genome Biol*. 8, R85.

Putnam, N.H., Srivastava, M., Hellsten, U., Dirks, B., Chapman, J., Salamov, A., Terry, A., Shapiro, H., Lindquist, E., Kapitonov, V. V., Jurka, J., Genikhovich, G., Grigoriev, I. V., Lucas, S.M., Steele, R.E., Finnerty, J.R., Technau, U., Martindale, M.Q., Rokhsar, D.S., 2007. Sea anemone genome reveals ancestral eumetazoan gene repertoire and genomic organization. *Science* 317, 86–94.

Rambaut, A., 2006. FigTree: tree figure drawing toolversion 1.4.4. Available at: http://tree.bio.ed.ac.uk/software/figtree.

Reddy, P.C., Unni, M.K., Gungi, A., Agarwal, P., Galande, S., 2015. Evolution of Hox-like genes in Cnidaria: Study of Hydra Hox repertoire reveals tailor-made Hox-code for Cnidarians. *Mech. Dev.* 138, 87-96.

Renfer, E., Amon-Hassenzahl, A., Steinmetz, P.R.H., Technau, U., 2010. A muscle-specific transgenic reporter line of the sea anemone, *Nematostella vectensis*. *Proc. Natl. Acad. Sci.* 107, 104–108.

Richards, T.A., Cavalier-Smith, T., 2005. Myosin domain evolution and the primary divergence of eukaryotes. *Nature* 436, 1113–1118.

Ruvkun, Gary, Hobert, O., Barnes, T.M., Jin, Y., Horvitz, H.R., Ruvkun, G, Hekimi, S., Neurochem, J., 1998. The Taxonomy of Developmental Control in *Caenorhabditis elegans*. *Science* 282, 2033–2041.

Ryan, J.F., Burton, P.M., Mazza, M.E., Kwong, G.K., Mullikin, J.C., Finnerty, J.R., 2006. The cnidarian-bilaterian ancestor possessed at least 56 homeoboxes: Evidence from the starlet sea anemone, *Nematostella vectensis*. *Genome Biol.* 7, R64.

Ryan, J.F., Mazza, M.E., Pang, K., Matus, D.Q., Baxevanis, A.D., Martindale, M.Q., Finnerty, J.R., 2007. Pre-bilaterian origins of the hox cluster and the hox code: Evidence from the sea anemone, *Nematostella vectensis*. *PLoS One* 2, 1–23.

Rychlik, W., Rhoads, R.E., 1989. A computer program for choosing optimal oligonucleotides for filter hybridization, sequencing and in vitro amplification of DNA. *Nucleic Acids Res.* 17, 8543-8551.

Salinas-Saavedra, M., Rock, A.Q., Martindale, M.Q., 2018. Germ layer-specific regulation of cell polarity and adhesion gives insight into the evolution of mesoderm. *Elife* 7, 1–28.

Satou, Y., Imai, K.S., 2015. Gene regulatory systems that control gene expression in the *Ciona* embryo. *Proc. Japan Acad. Ser. B Phys. Biol. Sci.* 91, 33–51.

Scherholz, M., Redl, E., Wollesen, T., Todt, C., Wanninger, A. 2015. From complex to simple: myogenesis in an aplacophoran mollusk reveals key traits in aculiferan evolution. *BMC Evol. Biol*. 201, 1-16

Schiemann, S.M., Børve, A., Hejnol, A., Martín-Durán, J.M., Passamaneck, Y.J., Vellutini, B.C., Børve, A., Vellutini, B.C., Passamaneck, Y.J., Hejnol, A., 2017. Clustered brachiopod Hox genes are not expressed collinearly and are associated with lophotrochozoan novelties. *Proc. Natl. Acad. Sci*. 114, E1913–E1922.

Schindelin, J., Arganda-Carreras, I., Frise, E., Kaying, V., Longair, M., Pietzsch, T., Preibisch, S., Rueden, C., Saalfeld, S., Schmid, B., Tinevez, J.Y., White, D.J., Hartenstein, V., Eliceiri, K., Tomancak, P., Cardona, A., 2012. Fiji: an open-source platform for biological-image analysis. *Nature Methods* 9, 676-682.

Seaver, E.C., 2014. Variation in spiralian development: Insights from polychaetes. *Int. J. Dev. Biol.* 58, 457–467.

Simionato, E., Ledent, V., Richards, G., Thomas-Chollier, M., Kerner, P., Coornaert, D., Degnan, B.M., Vervoort, M., 2007. Origin and diversification of the basic helix-loop-helix gene family in metazoans: Insights from comparative genomics. *BMC Evol. Biol.* 7, 1–18.

Song, M.H., Huang, F.Z., Gonsalves, F.C., Weisblat, D.A., 2004. Cell cycle-dependent expression of a *hairy and Enhancer of split (hes)* homolog during cleavage and segmentation in leech embryos. *Dev. Biol.* 269, 183–195.

Steffens, D.L., Sutter, S.L., Roemer, S.C., 1993. An alternate universal forward primer for improved automated DNA sequencing of M13. *Biotechniques* 15, 580

Sullivan, J.C., Reitzel, A.M., Finnerty, J.R., 2008. Upgrades to *StellaBase* facilitate medical and genetic studies on the starlet sea anemone, *Nematostella vectensis*. *Nucleic Acids Res*. 36, D607-D611

Sumner-Rooney, L.H., Sigwart, J.D., 2015. Is the Schwabe organ a retained larval eye? Anatomical and behavioural studies of a novel sense organ in adult *Leptochiton asellus* (Mollusca, Polyplacophora) indicate links to larval photoreceptors. *PLoS One* 10, 1–11.

Suzuki, M.M., Satoh, N., 2000. Genes expressed in the amphioxus notochord revealed by EST analysis. *Dev. Biol.* 224, 168-177.

Technau, U., Scholz, C.B., 2003. Origin and evolution of endoderm and mesoderm. *Int. J. Dev. Biol.* 47, 531-539

Thamm, K., Seaver, E.C., 2008. Notch signaling during larval and juvenile development in the polychaete annelid *Capitella sp*. I. *Dev. Biol.* 320, 304–318.

Thompson, R.F., Langford, G.M., 2002. Myosin superfamily evolutionary history. *Anat. Rec.* 268, 276–289.

Urano, A., Suzuki, M.M., Zhang, P., Satoh, N., Satoh, G., 2003. Expression of muscle-related genes and two *MyoD* genes during amphioxus notochord development. *Evol. Dev.* 5, 447–458.

Van Den Biggelaar, J.A.M., 1996. Cleavage pattern and mesentoblast formation in *Acanthochiton crinitus* (polyplacophora, mollusca). *Dev. Biol.* 174, 423–430.

Vega-López, G.A., Bonano, M., Tríbulo, C., Fernández, J.P., Agüero, T.H., Aybar, M.J., 2015. Functional analysis of Hairy genes in *Xenopus* neural crest initial specification and cell migration. *Dev. Dyn*. 244, 988–1013.

Wang, Jun, Zhang, Guofan, Fang, X., Guo, X., Li, L., Luo, R., Xu, F., Yang, P., Zhang, L., Wang, X., Qi, H., Xiong, Z., Que, H., Xie, Y., Holland, P.W.H., Paps, J., Zhu, Y., Wu, F., Chen, Y., Wang, Jiafeng, Peng, C., Meng, J., Yang, L., Liu, J., Wen, B., Zhang, N., Huang, Z., Zhu, Q., Feng, Y., Mount, A., Hedgecock, D., Xu, Z., Liu, Y., Domazet-Lošo, T., Du, Y., Sun, X., Zhang, Shoudu, Liu, B., Cheng, P., Jiang, X., Li, J., Fan, D., Wang, W., Fu, W., Wang, T., Wang, B., Zhang, J., Peng, Z., Li, Yingxiang, Li, Na, Wang, Jinpeng, Chen, M., He, Y., Tan, F., Song, X., Zheng, Q., Huang, R., Yang, Hailong, Du, X., Chen, L., Yang, M., Gaffney, P.M., Wang, S., Luo, L., She, Z., Ming, Y., Huang, W., Zhang, Shu, Huang, B., Zhang, Y., Qu, T., Ni, P., Miao, G., Wang, Junyi, Wang, Q., Steinberg, C.E.W., Wang, H., Li, Ning, Qian, L., Zhang, Guojie, Li, Yingrui, Yang, Huanming, Liu, X., Yin, Y., Wang, Jian, 2012. The oyster genome reveals stress adaptation and complexity of shell formation. *Nature* 490, 49–54.

Wanninger, A., Haszprunar, G., 2002. Chiton myogenesis: Perspectives for the development and evolution of larval and adult muscle systems in molluscs. *J. Morphol*. 251, 103–113.

Wanninger, A., Wollesen, T., 2015. Mollusca, in: Wanninger, A. (Ed.), Evolutionary developmental biology of invertebrates 2: Lophotrochozoa (Spiralia). *Springer Verlag*, Vienna, 103–146.

Waterhouse, A.M., Procter, J.B., Martin, D.M.A., Clamp, M., Barton, G.J., 2009. Jalview Version 2-a multiple sequence alignment editor and analysis workbench. *Bioinformatics* 25, 1189–1191.

Wells, L., Edwards, K.A., Bernstein, S.I., 1996. Myosin heavy chain isoforms regulate muscle function but not myofibril assembly. *EMBO J.* 15, 4454–4459.

Whelan, S., Goldman, N., 2001. A general empirical model of protein evolution derived from multiple protein families using a maximum-likelihood approach. *Mol. Biol. Evol.* 18, 691–699.

Wollesen, T., Scherholz, M., Todt, C., Redl, E., Wanninger, A., 2013. Aplacophoran mollusks evolved from ancestors with polyplacophoran-like features. *Curr. Biol*. 23, 2130–2134.

Yutzey, K.E., Rhee, J.T., Bader, D., 1994. Expression of the atrial-specific myosin heavy chain *AMHC1* and the establishment of anteroposterior polarity in the developing chicken heart. *Development 120*, 871–883.

Zhang, S., Bernstein, S.I., 2001. Spatially and temporally regulated expression of myosin heavy chain alternative exons during *Drosophila* embryogenesis. *Mech. Dev*. 101, 35–45.

Zusammenfassung

Das Mesoderm ist das jüngste der drei Keimblätter, welches sehr wahrscheinlich nach der Aufspaltung der Cnidaria und Bilateria entstand. Obwohl seine Morphogenese in vielen Metazoa gut untersucht ist, sind die molekularen Mechanismen der Mesodermbildung, in den meisten Phyla, weitgehend unbekannt. Dies trifft besonders auf den Stamm der sehr diversen Mollusca zu. Die Expressionsmuster der Gene *hairy and enhancer of split* (*HES*) und *Mox* wurden in *Acanthochitona*, einem Vertreter der Polyplcacophora, zusammen mit dem Myogenese Gen *Myosin heavy chain* (*MHC*), in dieser Studie untersucht. *AcaMHC* ist während der Myogenese in der frühen Larve, in den Muskeln der späten Larve und dem Juvenilen exprimiert. *AcaMox1* ist in den mesodermalen Bändern der frühen und in den ventrolateral Muskeln der späten Larve exprimiert. *AcaHESC2* ist in ektodermalen Zellen der Gastrula, in den mesodermalen Bändern der frühen Larve, und in, vermutlich, neuralen Gewebe der späten Larve exprimiert. *AcaHESC7* ist in den Trochoblasten der Gastrula und während der Entwicklung des larvalen Vorderdarms exprimiert. Die *AcaMox1* Expression in den mesodermalen Bändern ist ähnlich zu jener Expression in anderen Lophotrochozoen wie dem Gastropod *Haliotis asinina*, dem Brachiopod *Terebratalia transversa*, und dem Annelid *Alitta virens*. Ein Vergleich unter den Metazoa zeigt, dass *Mox* während der Mesodermentwicklung in vielen Metazoa (mit Ausnahme der Echinodermaten) und im Endoderm der Cnidaria exprimiert wird. Zusätzlich ist *Mox* in der Myogenese der Molluska, Annelida, Urochordata, und Craniata involviert, nicht jedoch in *Drosophila*. Nematoda haben ihr *Mox* Ortholog generell verloren. *HES* Gene werden in mehreren Entwicklungsprozessen exprimiert wie der Segmentierung, Neurogenese, und Entwicklung des Verdauungstraktes. Somit sind so genannte mesodermale Gene nicht nur auf die Mesodermbildung allein beschränkt. Weitere Studien sind notwendig, um die molekularen Einflüsse der Mesodermentwicklung in Bilateriern zu verstehen.